Czech Technical University in Prague

Faculty of Civil Engineering

Department of steel and timber structures

Master's Thesis

The influence of the residual stresses on the static behaviour of the rail

Student: Andrei Stadnik

Supervisor: Doc. Ing. Pavel Ryjáček, Ph.D.

Study Program: Sustainable Construction Under Natural Hazards and Catastrophic Events (SUSCOS)

Field of Study: Civil Engineering

CVUT

January 8, 2017

CZECH TECHNICAL UNIVERSITY IN PRAGUE
Faculty of Civil Engineering
Thákurova 7, 166 29 Prague 6, Czech Republic

DIPLOMA THESIS ASSIGNMENT FORM

I. PERSONAL AND STUDY DATA

Surname: Stadnik Name: Anrej Personal number:

Assigning Department: Department of steel and timber structures

Study programme: CIVIL ENGINEERING

Branch of study: SUSCOS

II. DIPLOMA THESIS DATA

Diploma Thesis (DT) title: Vliv reziduálního pnutí na statické chování kolejnice

Diploma Thesis title in English: The influence of the residual stresses on the static behaviour of the rail

Instructions for writing the thesis:
- to create the nonlinear material model with the residual stresses pattern,
- to perform the load test on the rail,
- to evaluate the results,
- to analyze the impact of the residual stresses in the rail in the track

List of recommended literature:
MVL 150 - Mostní vzorový list interakce most a kolej
UIC 774-3
ČSN EN 1991-2

Name of Diploma Thesis Supervisor: doc. Ing. Pavel Ryjáček, Ph.D.

DT assignment date: 9.10.2016 DT submission date: 8.1.2017

[redacted] [redacted]

DT Supervisor's signature Head of Department's signature

III. ASSIGNMENT RECEIPT

I declare that I am obliged to write the Diploma Thesis on my own, without anyone's assistance, except for provided consultations. The list of references, other sources and consultants' names must be stated in the Diploma Thesis and in referencing I must abide by the CTU methodological manual "How to Write University Final Theses" and the CTU methodological instruction "On the Observation of Ethical Principles in the Preparation of University Final Theses".

09 10 2016 [redacted]

Assignment receipt date Student's name

DECLARATION

This dissertation is the result of my own work and includes nothing, which is the outcome of work done in collaboration except where specifically indicated in the text. It has not been previously submitted, in part or whole, to any university of institution for any degree, diploma, or other qualification.

Signed: _____

Date: 08.01.2017

Andrei Stadnik

ABSTRACT

The issue of track-bridge interaction is relatively broad and includes wide range of input parameters, which are currently under investigation as part of research projects focused on this problem. Measurement of existing bridge structures, rails, numerical models and so forth are under investigation.

One of the parameters that have an influence on longitudinal resistance of the rail is the residual stress field in it. For the past years residual stresses were under investigation mainly because they have a big influence on the fatigue resistance of the rail which is one of the failure modes for the steel rail.

The primary purpose of this study is to investigate the influence of the residual stresses on flexural behaviour of the rail.

Bending resistance of two specimens will be experimentally studied: new rail with residual stresses and heat treated piece with relieved residual stresses. Finite Element Model (FEM) will be developed to simulate the test.

Map of residual stresses is introduced in numerical model of the rail and it is based on the evaluation and analysis of a number of researches that were done in this area. In order to check compatibility of the chosen pattern with our specimens, residual stresses in an additional - third specimen will be checked according to simplified procedure described in EN 13674-1 Annex C.

Keywords: Track-bridge interaction, Rails, Residual stresses, Flexural behaviour

ACKNOWLEDGEMENTS

Immeasurable appreciation and deepest gratitude for the help and support are extended to the following persons who in one way or another have contributed in making this study possible.

Doc. Ing. Pavel Ryjáček, Ph.D, my thesis supervisor, for his support, guidance, valuable advices and suggestions that benefited me much in the completion of the current study. His mentorship has enriched my knowledge in the scope of railway engineering. Continuous support made this thesis work go smoothly and last an endless help to finish it.

Doc. Ing. Jiří Litoš, Ph.D and staff of the Experimental Centre CVUT for the kind effort to arrange and execute the test. Special thanks goes to laboratory technician **Jan Slouka** for his explanations and help during and after the test.

I would like to thank my classmates for their lively interest in my thesis topic and interesting discussions we had.

Additional gratitude goes to Erasmus Mundus Program for the given opportunity.

CONTENTS

LIST OF TABLES

LIST OF FIGURES

LIST OF ANNEXES

1 INTRODUCTION

A railway bridge may support a load of several hundred tons in midair. The load is transmitted through various parts of the structure to the foundations, where it dissipates into the ground. You might not think of the track itself as a structure but in fact it does a similar job on a smaller scale.

Here, the structure consists of three main elements: rails, sleepers and road bed. They work together to support the wheels of a moving train, and spread out the load underneath.

The engineer's task is to work out the cheapest possible configuration that meets following requirements. First, the rails mustn't break, and second, any deflection under the wheels of a train should fall within an acceptable range: too much and a train may jump the rails, too little and the track will provide a rough ride and wear out prematurely.

Introduction of the bridge as a supporting structure brings another requirement: rail mustn't break due to longitudinal forces appearing from track-bridge interaction.

Conventional shape of railway rail basically didn't change since the day of invention. It is determined by the dual function the rail performs:

- Rail is supporting and load-distributing element of the permanent way
- Rail provide vehicle guidance

The requirements imposed upon the rail led to the present cross-sectional shape: a relatively heavy upper part, the "head", narrow intermediate part, the "web", and a wide bottom flange, the "foot". Since cross-section is non-rectangular, the one can assume that stress distribution differs from classic beam theory [1]. Moreover, residual stresses are introduced in rail as a sequence of the production process.

What is more, forces acting on rail vary in direction:

- Vertical – due to wheel dead load
- Horizontal (normal to longitudinal direction) – due to centrifugal forces
- Longitudinal – thermal and due to track-bridge interaction

Therefore bearing capacity of the rail depends on many factors.

Scientific research doesn't always lead to developing new materials, sections, etc., but it also leads to the more complete usage of already existing elements.

In order to illustrate that idea European and Russian steel design codes can be considered. While SNIP is more conservative and assumes only elastic behaviour (elastic global analysis), EC tends to the complete utilization of the properties of steel and allow plastification of some parts (plastic global analysis for certain types of sections). That was a result of thorough research of both theoretical and experimental data, as a conclusion it was stated that plastic global analysis allows forming plastic hinges and consequent redistribution of forces for other sections (with lower forces).

Similarly, railway rail can be studied in terms of its bearing capacity. Cross-sectional shape of it almost didn't change in past 100 years, although demands are growing: continuous welded rail technology, increasing spans of bridges, increasing speed of the trains, etc.

Purpose of the current paper is to investigate the influence of residual stresses in rail on its longitudinal resistance. Rail profile UIC60 (60E1) is investigated.

2 STATE-OF-ART

2.1 Track-bridge interaction

2.1.1 Principles of stress generation

In old times, the tracks were built only as the rail pieces of lengths up to 25 m. This allowed free expansion of the rail to a certain temperature rails, and consequently longitudinal stresses due to temperature variation were not created.

The track contact induces additional dynamical impact on the rail that leads to increased wear of the rail, vibrations and noise, which also reduce comfort of passengers. Developing procedures for welding rails has gradually switched to the establishment of continuously welded rail tracks (CWR). When the vehicle is traveling on CWR track, there is no dynamic impact on the rail contacts, which increases comfort, reduces dynamic loading acting on railway superstructure and substructure, reduces maintenance costs of the track, increases safety on the track, and consequently leads to lower operational costs.

On other hand, introduction of CWR brings additional requirements in railway design. In a traditional ballasted track, rails are fastened to the sleeper by elastic fastenings with predefined clamping force. This force is generally high enough to consider that the longitudinal movement of the rail is transmitted to the sleepers. In other words, the resistance to rail-sleeper sliding is greater than the resistance to longitudinal movement offered by the ballast. As the free movement of the rail is opposed by the ballast under the thermal and traffic load, the rails are therefore subjected to longitudinal forces.

Introduction of a bridge as a substructure for the track brings additional source of loadings acting on a rail. As both track and bridge are able to move, any force or displacement that acts on one of them will induce forces in the other. Interaction therefore takes place between the track and the bridge as follows [2]:

- Forces applied to a CWR track induce additional forces into the track and/or into the bearings supporting the deck and movements of the track and of the deck;
- Any movement of the deck induces a movement of the track and an additional force in the track and, indirectly, in the bridge bearings.

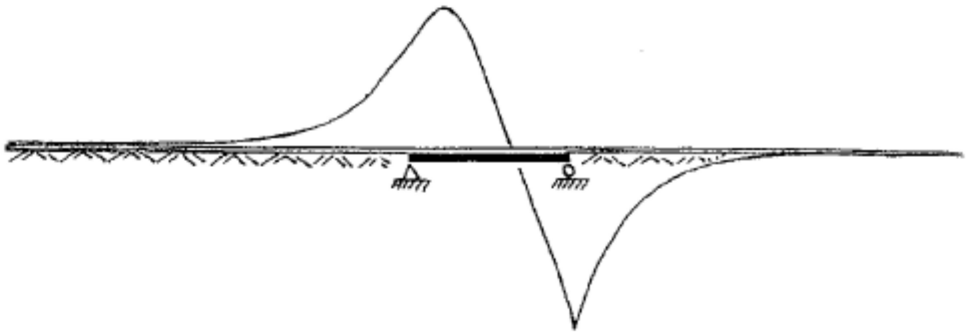

Figure 1. Example of a curve showing rail stresses due to temperature variations in the bridge deck

2.1.2 Design rules for accounting track-bridge interaction

2.1.2.1 Leaflet UIC 774-3 and EN 1991-2

Leaflet UIC 774-3 and prescriptions listed in EN 1991-2, 6.5.4 deal with the issue of track-bridge interaction.

Standard includes following parameters for the track-bridge interaction, 6.5.4.3 – Actions to be considered:

- Traction and braking forces;
- Thermal effects in the combined structure and track system;
- Classified vertical traffic loads;
- Other actions such as creep, shrinkage, temperature gradient etc. shall be taken into account for the determination of rotation and associated longitudinal displacement of the end of the decks where relevant.

For rails on the bridge and on the adjacent abutment the permissible additional rail stresses due to the combined response of the structure and track to variable actions should be limited to the following design values:

- Compression: 72 N/mm^2,
- Tension: 92 N/mm^2.

According to UIC 774-3, permissible limit values given are the values that are widely permitted for standard track components in a good state of maintenance. If a railway operates outside foreseen scope of application, that railway will still be able to use the calculation methods in this leaflet by replacing the criteria given above with new criteria based on its own experience and observations.

The limiting values given by EN 1991-2 are valid for the track complying with:

- UIC 60 rail with a tensile strength of at least 900 N/mm²,
- straight track or track radius r >1 500 m,
- for ballasted tracks with heavy concrete sleepers with a maximum spacing of 65 cm or equivalent track construction,
- for ballasted tracks with at least 30 cm consolidated ballast under the sleepers.

Therefore taking into account track-bridge interaction according to the bridge design procedure provided by EN 1991-2 implies the adoption of a number of simplifications, which greatly limits its wider use. The standard is missing another uniform procedure for the cases where assumed conditions are not met.

2.1.2.2 MVL-150

The reason for establishing new methodology is the absence of normative documents on the issue, which would address to a wider range of possible cases.

The proposed technical solutions of the bridge structures (especially bridges with large expansion length) are often intend to operate at the limit of technical possibilities of materials, structural design and geotechnical conditions. In order to effectively deal with such complex cases of bridge structures it is needed to develop methodology that enables the optimization of bridge design. The unification of the design methods in the standard will contribute to increasing the safety of the railway infrastructure, enhancement of the effectiveness of the technical solutions for the bridge structure, reduction of investment costs for bridge construction and, last but not least, reduction of the negative impact of rail transport on the environment.

As part of the national annexes to EN 1991-2 adjustments to the existing design procedure were made so that it is possible to perform an analysis of the combined response of the structure and rails according to alternative design criteria. Alternative design criteria are based on the principles set out in EN considering the conditions of operation of the railway in the Czech Republic.

Combined response of the structure and the track can be analysed using a method called "Complete analysis". This method is general and it can deal with almost any arrangement of the bridge and any types of rails on the bridge. On the other hand, it is time consuming.

The main idea of the entire analysis is to assess the overall stress in rail according to condition prescribed in EN 1993-2 6.2.10.2 Resistance of cross-sections, Bending and axial force.

In determining of the total stress in rail, these sub-stress components are considered [[3]]:

- Residual stresses from production: □□
- Stress from temperature changes of track in the track: □□
- Stress from temperature changes of the bridge: □□
- Power from braking and the traction forces: □□
- Stress from the vertical effects of local traffic load on the bridge: $\square_{P.lok}$
- Stress from the vertical effects of global traffic loads on the bridge: $\square_{P.glob}$

Graphical representation of the individual components of the stress is shown on the picture below [3] (Figure 2).

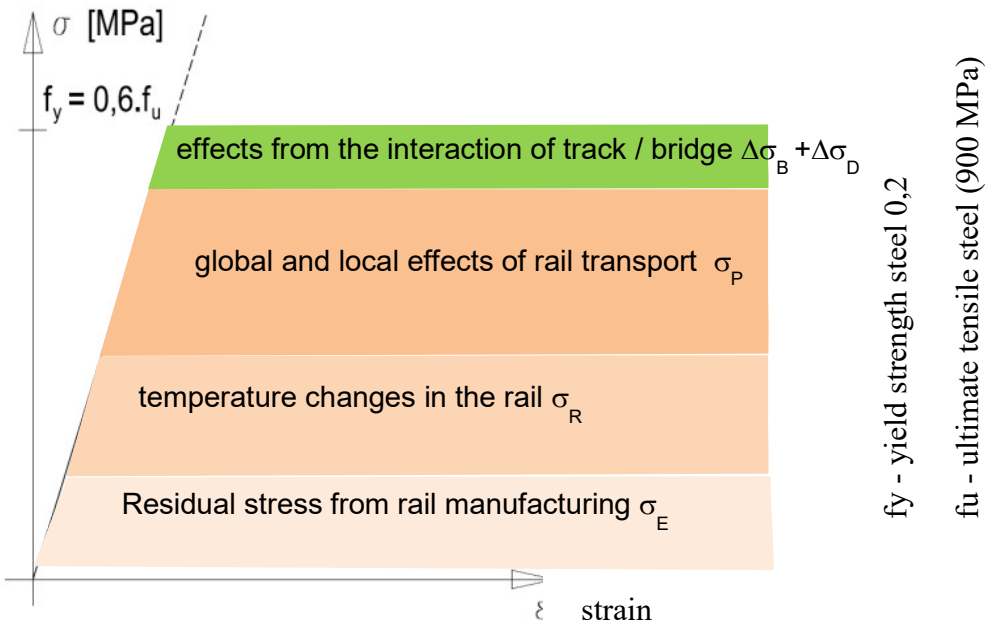

Figure 2. Stress components in railway rail

When the total stress rail $\square\square_{,i}$ is calculated, following relationship from EN 1993-2 Art. 6.2.10.2 for Class 3 cross section can be used:

$\square\square_x < f_{y,k}/\square_{M0}$

2.2 Residual stresses in railway rail

Residual stresses are important to security and comfort in railway traffic. Their value can be significant and have an influence on overall design of the track-bridge system as it was showed in previously - Figure 2. Stress components in railway rail.

The most critical point here is the foot, where longitudinal tensile stresses due to the wheel loads and tensile residual stresses superimpose.

Due to increasing speed and rising wheel loads of freight cars, more and more research interests have been directed to the railway system and now railway administrations demand straightness and low tensile residual stresses in the foot. It is done mainly to improve crack growth - fatigue resistance. Wear, and thus maintenance costs, are influenced by residual stresses.

2.2.1 Formation of residual stresses

The production of rail consists of three steps:

1. Hot rolling
2. Cooling
3. Straightening

Residual stresses develop on each step. “Residual stress formation and distortion of Rail steel” [4] presents an overview of the studies that were carried concerning developing of residual stresses during all the stages of production.

It was proven both numerically and experimentally that the last step – straightening process has the biggest influence on residual stress pattern in the rail. For example, residual stress state due to cooling is fully eliminated during the straightening process.

Authors investigate processes occurring at each stage. As the main reason why the rail need to be straightened is its curvature after the cooling process, one needs to understand the nature of obtaining that shape and if there is a way to reduce the curvature as much as possible.

After rolling, the temperature in the rail is higher than 900° C and it is assumed to be spatially constant over the entire cross section at the beginning of the cooling procedure. Cutting and transportation take usually about 4 min until the rail reaches the cooling area.

The mass distribution along the axis of symmetry of rail varies significantly. The rail head represents a mass concentration of a roughly square shape. However the web and the foot can

be approximated by plates. Therefore the cooling process of a rail profile with an initially spatially constant temperature distribution results in a strong inhomogeneous temperature field and a thermal stress state. If the rail is free from external constraint, of course, neither a resultant moment nor a resultant force can appear due to pure cooling. Most of the rails cool down with contact and thermal interactions with neighbouring rails that can be seen on Figure 3. In this process, the longitudinal shape of the rail changes due to different cooling speeds of its different parts.

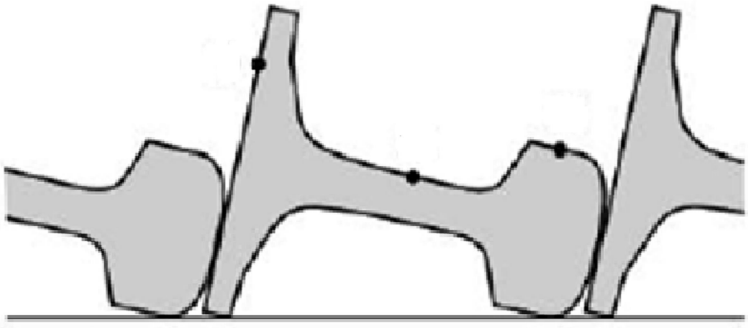

Figure 3. Rails on the cooling bed

Since there are certain requirements for the rail straightness, a further production step – straightening is conducted. Although several techniques for rail straightening presents, roller straightening is the most used one. Because it allows continuous operation for long products, it is the fastest method. The cool, distorted rails are drawn through the straightener by a series of driven rollers, which are located alternately below and above the rail. While the rail is passing through the rollers in the longitudinal direction, it is bent up and down. Thus, the initial distortion is homogenized and decreased by the plastic deformation caused by combination of bending, shear, and roll contact stresses.

The usual profile of longitudinal residual stresses after straightening is a C-shaped curve, where both the head and the foot of the rail are subjected to longitudinal tensile residual stresses, while the web of the rail is subjected to compression forces. Several researchers came up with same result [6], [7], [8]. This profile of residual stresses is unfavourable when the rail is in service, since the operation stresses taken in conjunction with the residual stresses can cause the appearance of cracks and their subsequent growth by fatigue.

The most critical point is a rail foot, as it was mentioned before. According to EN 13674-1 residual stress in the foot should not exceed 250 MPa.

Residual stresses arisen after production process evolve during service life of the rail, as a result of the wear and plastic deformation that occurs at the running surface. The most

noticeable change in residual stress during service is the formation of a region near the running surface, extending up to 20 mm into the rail head, which contains compressive residual stress in those directions parallel to the running surface. [8]

2.2.2 Experimental investigation of residual stresses in rail

Both experimental and numerical investigations have been carried out in the past to reveal the formation of dominant longitudinal residual stresses.

Experimental investigation of residual stresses in rail can be divided in two groups:

1. Destructive (including semi-destructive)
2. Non-destructive

2.2.2.1 Sectioning technique

Sectioning technique is a destructive method that relies on the measurement of deformation due to the release of residual stress upon removal of material from the specimen.

According to a European Committee for Standardization (CEN) – Annex C of EN 13674-1, the measurement of tensile residual stress in the rail foot has to be performed in the following way: a strain gage is attached in longitudinal direction in the middle of the rail foot. Then, a saw cut in front of and behind the gage position and normal to the longitudinal direction relieves the residual stresses. The stress relief causes an elastic strain, which can then be measured by the strain gage. Finally the original longitudinal stresses can be calculated by multiplying by the Young Modulus 210 GPa.

Extensive investigation work has been carried out in past years. Most of the experimental tests have shown C shape pattern of residual stresses in rail cross section.

The sectioning method performed by ORE [10] consists of making a cut on an instrumented plate in order to release the residual stresses that were present on the cutting line. The strains released during the cutting process are generally measured using electrical or mechanical strain gages. Hodgson [11] summarized results made by ORE and obtained a scatter band of the longitudinal stresses in rail.

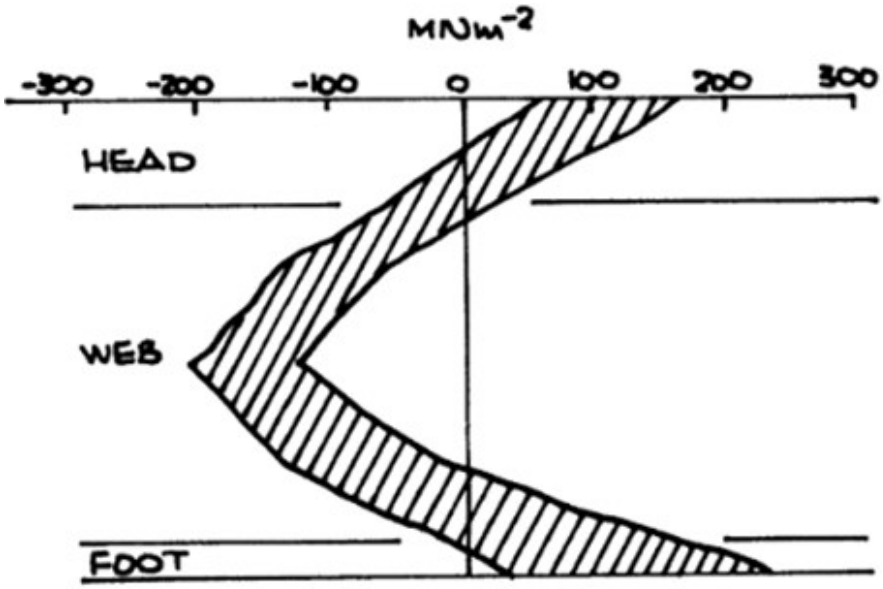

Figure 4. Scatter band of longitudinal residual stresses measured by ORE [10] in unused roller straightened rail

2.2.2.2 Neutron diffraction method

PJ Webster [7] used neutron diffraction method for investigation. It is a non-destructive method. Neutrons can penetrate in metal, allowing the measurement of residual stresses in the interior of the material, though only on a depth of up to 25 mm in steel.

Since metals are composed of atoms arranged in a regular three-dimensional array to form a crystal, most metal components of practical concern consist of many tiny crystallites (grains), randomly oriented with respect to their crystalline arrangement and fused together to make a bulk solid. When such a polycrystalline metal is placed under stress, elastic strains are produced in the crystal lattice of the individual crystallites. In other words, an externally applied stress or residual one within the material, when bellow the yield strength of the material, is taken up by inter-atomic strains in the crystals by knowing the elastic constants of the material and assuming that stress is proportional to strain, a reasonable assumption for most metals and alloys of practical concern. Diffraction can directly measure inter-planar atomic spacing; from this quantity, the total stress on the metal can then be obtained.

Investigation was done on a new and used rail. Results are presented together with results from ORE [10] cutting method.

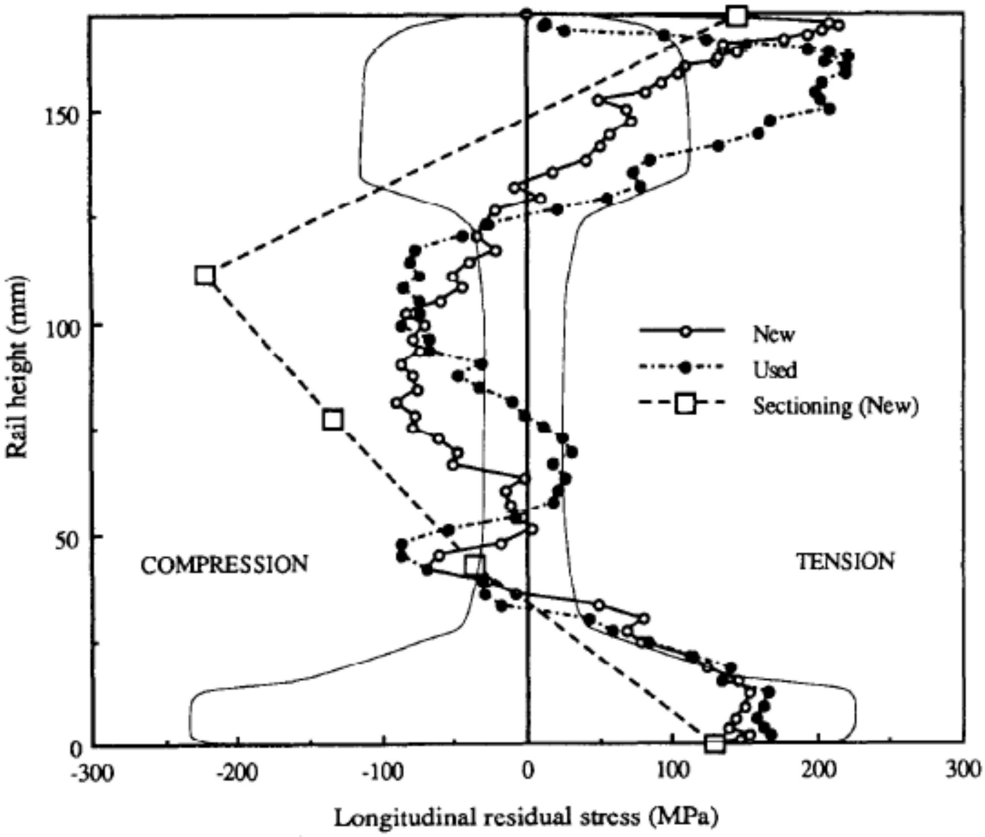

Figure 5. Longitudinal residual stresses down the centre line of new and used head hardened rails measured by neutron strain scanning and sectioning techniques

2.2.2.3 Contour method

Contour method is an advanced sectioning method [8]. It is a newly invented relaxation method that enables a 2D residual stress map to be evaluated on a plane of interest. First papers were presented in 2000. Therefore, consensus best practices are not as well established as for other methods. The contour method determines residual stress through an experiment that involves carefully cutting a specimen into two pieces and measuring the resulting deformation due to residual stress redistribution. The measured displacement data are used to compute residual stresses through an analysis that involves a finite element model of the specimen. As part of the analysis, the measured deformation is imposed as a set of displacement boundary conditions on the model. The finite element model accounts for the stiffness of the material and part geometry to provide a unique result. The output is a two-dimensional map of residual stress normal to the measurement plane.

Investigation was done on a two specimens of 113A rails: new roller-straightened rail and one that had undergone 23 years of service. The resulting stress maps were presented. Maps showed that the residual stresses are tensile in the head and foot of the rail, with the peak

stresses located subsurface. There are balancing compressive stresses in the web and in the lateral regions of the foot.

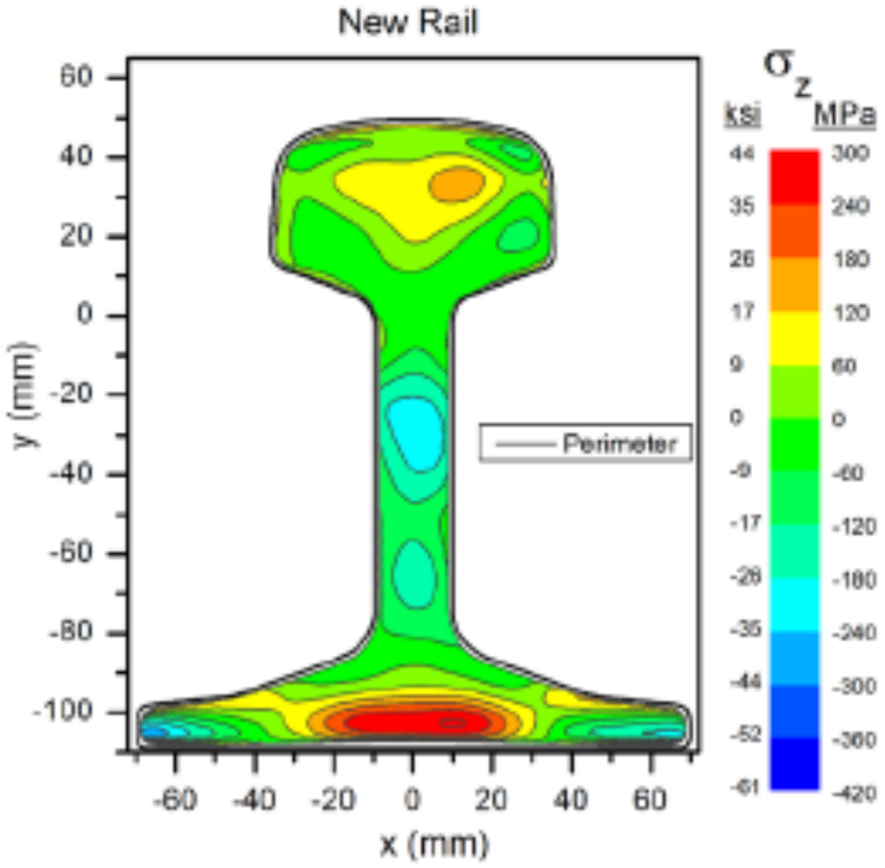

Figure 6. Map of residual stresses in unused 113A rail

2.2.2.4 Incremental centre-deep hole drilling technique (IC-DHD)

Group of scientists from UK [6] measured residual stresses using an integrated drilling technique in UIC60 rail. Proposed technique is a development of the semi-destructive hole-drilling. Hole-drilling method is relatively simple and fast and can provide the measurement of residual stress distribution across the thickness in magnitude, direction and sense. It has the advantages of good accuracy and reliability, standardized test procedures, and convenient practical implementation. The damage caused to the specimen is localized to the small, drilled hole, and is often tolerable or repairable. The principle involves introduction of a small hole (of about 1.6 mm diameter and up to about 2.0 mm deep) at the location where residual stresses are to be measured. Due to drilling of the hole the locked up residual stresses are relieved and the corresponding strains on the surface are measured using suitable strain gages bonded around the hole on the surface.

In the deep-hole drilling method, a hole is first drilled through the thickness of the component. The diameter of the hole is measured accurately and then a core of material around the hole is trepanned out, relaxing the residual stresses in the core. The diameter of the hole is re-measured allowing finally the residual stresses to be calculated from the change in diameter of the hole. The main feature of the method is that it enables the measurement of deep interior stresses and allows non-uniform stress profiles to be measured.

This procedure carries out both bulk and near surface residual stress measurement in rails. While being able to measure accurately through-thickness residual stresses in the bulk of thick components, the accuracy of the DHD technique near to the surface is uncertain. Using the CHD technique provides a reasonable solution for surface residual stresses. Authors came to the conclusion that application of the CHD technique prior to DHD technique does not affect the latter, hence usage of two techniques combined is beneficial.

At the foot (Z=0) and at the head (Z=172mm) of the rail the longitudinal residual stresses were similar, approximately 15MPa. The longitudinal residual stresses measured by IC-DHD were compared with neutron diffraction technique [7] and good agreement between them was found.

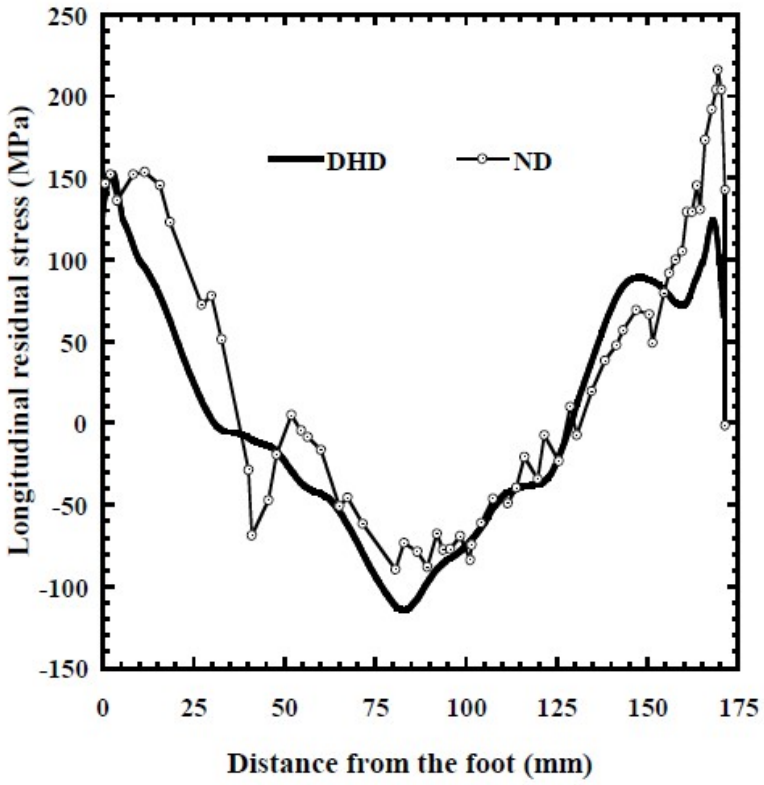

Figure 7. Comparison between the DHD and neutron diffraction longitudinal

2.2.3 Numerical modelling of residual stresses in rail

Different FE analyses were performed to predict residual stress prediction in rails. The studies of F.D. Fischer and G.Schleinzer [4] summarize the previous attempts on modelling of formation of residual stresses in the rail:

"Different attempts were made to simulate the roller straightening. Brunig used beam elements of different widths accounting for the special cross section of the rail. He already used an enhanced two-surface plasticity model. Because elements covering the whole width do not allow a variation of stresses along the width, his results are, at best, average values. He also stated that the contact pressure at the rollers had only a minor influence on the residual stresses. Naumann investigated a full three-dimensional FEM model with an explicit integration method, a coarse mesh, and linear kinematic hardening. However, he did not publish residual stress results from his calculations. In contrast to Brunig, Naumann stated that the pressing of the rollers into the rail head and foot is in fact responsible for the residual stress pattern. Weiser applied straightening mechanics on a slice of rail. He implemented the roller contact with an overlay of Hertz-type contact pressure. The results correspond qualitatively with the measurements. Finstermann applied moments and forces of a beam model on a three-dimensional FEM model of a piece of rail in order to bend it around a top and bottom roller. The repeated contact with the top and bottom roller was supposed to give a good approximation of the real roller contact. The results show compressive stresses at the head and foot surface that are much higher than the ones hinted at in the measurements of Webster or Hauk. Varney again used a beam model with a linear kinematic hardening law. The result is a zig-zag pattern of longitudinal stresses. Henderson modelled the process by a series of three-point bendings and linear kinematic hardening. A first result had only little resemblance to measured U- (or C–) shaped patterns. After the material parameters had been adjusted to unstraightened and straightened conditions, the simulation gave better results."

The authors employed a procedure with a minimum simplifications in their model. In order to save computational time, the model was split in two: global model – 16m long with a coarse mesh and linear kinematic hardening law; submodel – less than 1m long with a fine mesh and multiple component hardening model of Chaboche [12]. Driving of the specimen in submodel was controlled by the nodal displacement of the global model.

The result of this simulation showed a C-shaped residual stress pattern (Figure 8). As the authors concluded, the results fit at least qualitively to experimental evaluations [7].

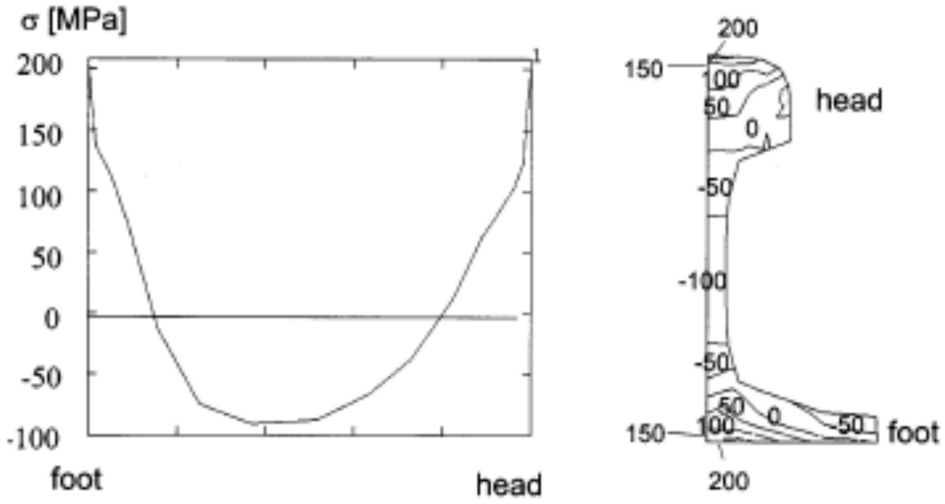

Figure 8. Longitudinal residual stresses after the straightening in MPa along the symmetry line and as a contour plot.

2.3 Investigation of the stresses in rails due to bending

Research on the stress distribution in a flexurally loaded rail was undertaken by researchers in Netherlands in 1982 [14]. For this purpose analytical studies, experiment and numerical model were developed.

Analytical studies are based on the work of Timoshenko S. dedicated to development of stresses in railroad rail [1] and on the system of mechanical relationships developed by Prof. Dr. Ing. J. Eisenmann, Technological University of Munich, and other investigators which describe flexural behaviour of a rail under centric loading [15]. Large tensile stress under the head was predicted to occur in the cross-section where the vertical is applied. The reason for that is secondary bending that appeared due to the shape of the rail.

A rail of NP 46 section was subjected to experimental research with the aid of electrical resistance strain gauges.

Our particular interest is the numerical model that was developed in research. Flexural stresses in the rail due to centric load were analysed with the ICES/STRUDL application package, by means of the IBM 360 computer. There is no information about initial stresses in the model, so it can be assumed that they were not incorporated in the model. Same conclusion could be made also considering year when the research was done – 1982. Authors describe capabilities of the program, which a quite limited comparing to what is available now.

Authors studied behaviour for the loading case with F=100 kN and a span of 700 mm. They found good agreement between experimental and numerical results (Figure 9). Existence of tensile stresses under the head was confirmed. Although it was found that the phenomenon of secondary bending is very local in character. At a distance of about 60 mm in the axial direction from point of load application an approximately linear stress distribution is already found.

Considering that residual stresses do exist in test specimen and they were not introduced in the numerical model, it can be concluded that no significant influence of residual stresses on flexural behaviour of the rail occurred.

Future development of numerical modelling was proposed.

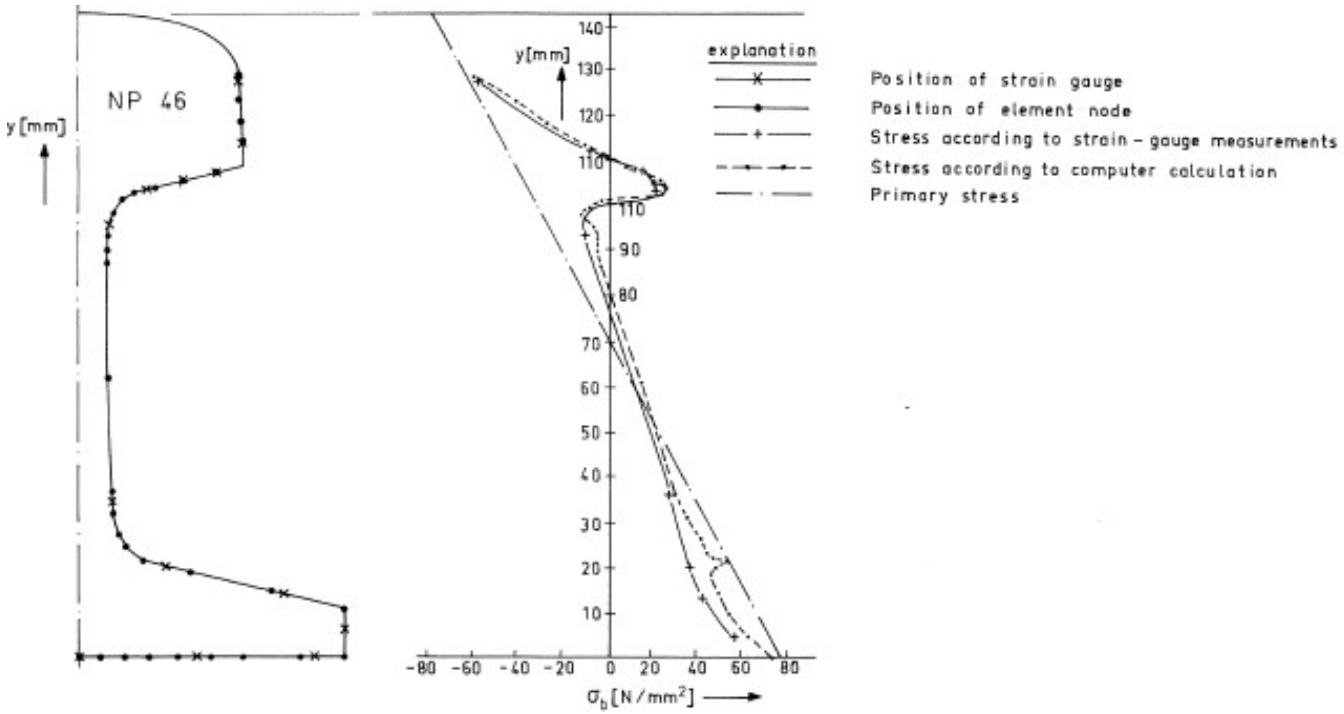

Figure 9. Flexural stresses in the cross-section in which the point of load-application occurs

3 OBJECTIVES

The primary purpose of this study is to investigate the influence that residual stresses in the rail have on the resistance of the rail.

The transverse bending test is frequently employed until fracture or yielding in the specimen and in that case is used for studying nonlinear behaviour particular to members made of ductile materials. The main advantage of the flexural test is the ease of the specimen preparation and testing. However, this method has also some disadvantages: the results of the testing method are sensitive to specimen and loading geometry.

Primary objectives can be divided into following particular objectives:

- To carry out bending test of the railway rail
- To measure residual stresses in rail
- To validate FEM of the rail in bending
- To estimate influence of residual stresses on the bending capacity of the rail

4 BENDING TEST

4.1 Preparation for the test

4.1.1 Goal of the test

Member made of ductile material and subjected to bending load exhibit elastic-plastic bending. In both elastic and plastic analyses it is assumed that plane sections remain plane. In an elastic analysis this assumption leads to a linear stress distribution, but in a plastic analysis the resulting stress distribution is nonlinear. In other words cross-section doesn't become plastic at once. In the absence of strain hardening, the maximum moment which can be sustained occurs when every fibre of the section has yielded. First yielding occurs in outermost fibres which progresses with increasing of bending moment. The yielded areas of the cross-section will vary somewhere between the yield and ultimate strength of the material exhibiting behaviour that is known as plastic bending (Figure 10).

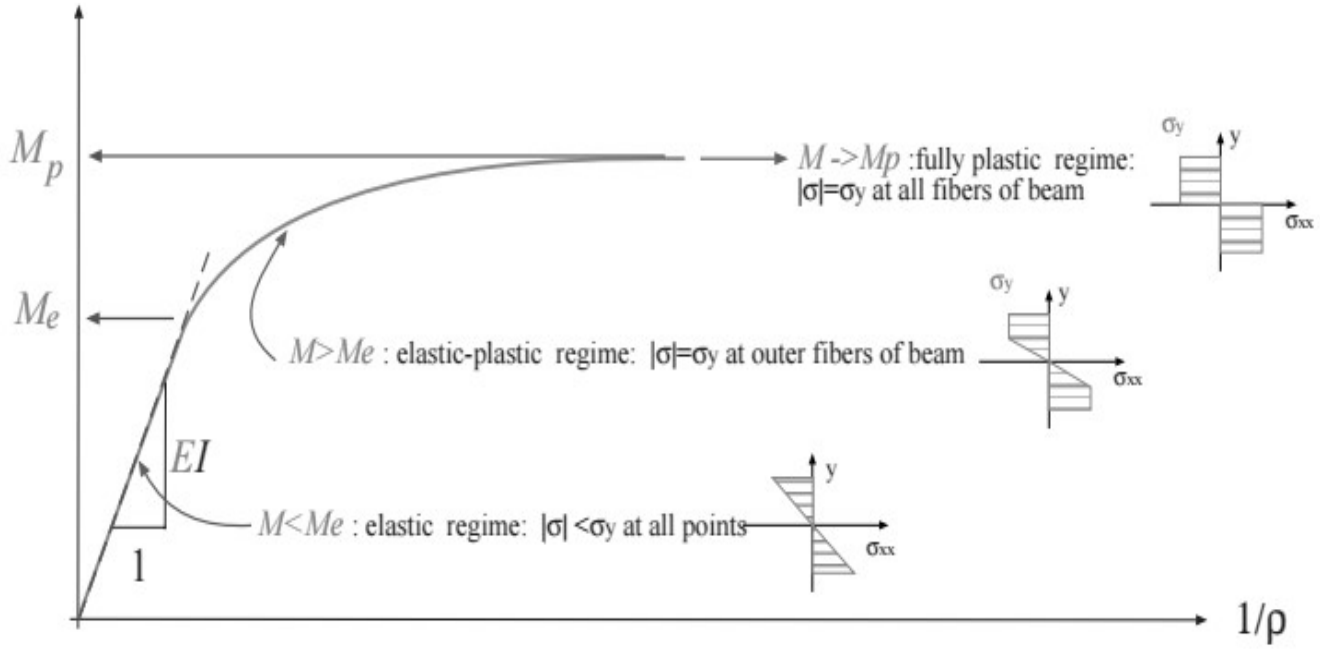

Figure 10. Bending moment – Curvature of the bended beam relationship

Several factors can affect distribution of stresses in cross section in plastic bending: material properties (stress-strain relationship for uniaxial tension and compression, strain

hardening), symmetry of shape and presence of residual stresses. Plastic bending causes complex stress distribution where presence of residual stresses can be studied.

Plastic moment Mp can be considered as an upper limit to a beam's load–carrying capacity. Although a beam may fail due to global or local instability before Mp is reached at any point on its length. Therefore, beams should also be checked for local and global lateral–torsional buckling.

Four-point bending is beneficial to three-point bending for the following reasons:

- It is possible to apply strain gauge on the top of the rail
- Secondary bending effect is avoided (2.3)

4.1.2 Preparation of the samples

4.1.2.1 Susceptibility to buckling

It was already mentioned in paragraph above that failure of the beam can occur due to local or global buckling. EN 1993-1 provides classification of cross-section according to their susceptibility to lateral buckling. Railway rail is considered as a beam and required calculation for a section classification can be adopted. Load is planned to be applied on the rail top, thus it is going to be in compression. Obviously shape of rail head makes it is not susceptible to lateral-torsional buckling due to bending. Consequently no lateral supports should be added to the test layout.

In order to capture possible local buckling of the web, two strain gauges shall be applied on both sides of the web.

4.1.2.2 Required length

EN 13674-1 specifies length of the specimen for residual stress measurement as 1m, so stresses can be measured in the middle of the piece. Therefore 1 m can be considered as the minimum length of the test specimens for bending tests.

Laboratory equipment has a capacity of 1.5 MN. In order to reach plastic moment, required length of the specimen should be calculated.

Dimensions and main geometric properties of the rail are presented in Annex 1.

Additional geometric properties (Table 1) were calculated in LTBeam with the use of simplified rail section (Figure 10). LTBeam is software which deals with "Lateral Torsional Buckling of Beams" under bending action about their major axis.

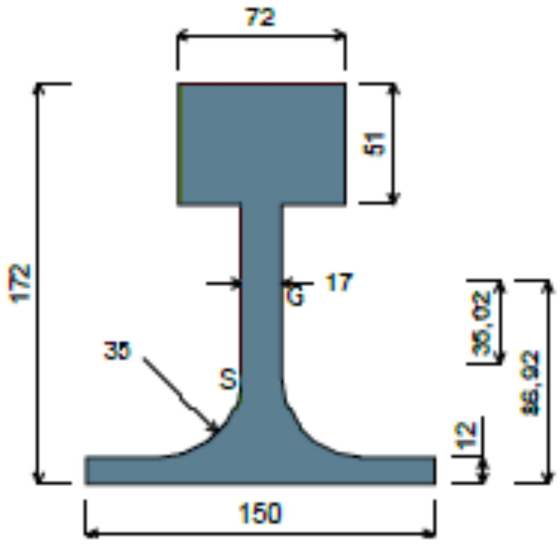

Figure 11. Simplified rail section in LTBeam (dimensions in mm).

Table 1. Geometrical properties of the rail.

Geometrical properties	EN 13674-1:2011	LTBeam
Moment of inertia (major axis), I_{xx} [cm^4]	3038.30	3063.6
Elastic section modulus, w_{el} [cm^3]	-	360.1
Plastic section modulus, w_{pl} [cm^3]	-	451.1

S260 steel properties:

Tensile strength $f_u := 900MPa$

Yield strength $f_y := 0.6 \cdot f_u = 540 \cdot MPa$

Elastic and plastic moments are then:

$M_{el} := w_{el} \cdot f_y = 194.4 \cdot kN \cdot m$

$M_{pl} := w_{pl} \cdot f_y = 243.6 \cdot kN \cdot m$

Calculating minimum length of the specimen:

Moment in the middle of the span for four-point bending:

$$M = \frac{F \cdot (L - L_i)}{4}$$

Where Li is distance between load application points $L_i := 0.2m$

$M := M_{pl} = 243.6 \cdot kN \cdot m$

Capacity of the equipment in the laboratory (reduced for the sake of safety): $F := 1MN$

Minimum length of the rail is then $L := \frac{4 \cdot M}{F} + L_i = 1.17\,m$

Final length of the rail specimens is chosen to be 2m. Considering that length residual stresses should remain constant over the middle part of the specimen. What is more installation is simple in case of the specimen being longer than distance between supports that allows rail to slip for the high bending angles.

4.1.2.3 Heat-treatment

One of the test samples was heat-treated before the experiment. This procedure is needed for the releasing of residual stresses raised from manufacturing process. It was done by the company “Bodycote”. “Bodycote” is one of the most experiences companies in the world that provide thermal processing services.

Stress relieving might not change the material’s. The stress relieving temperature is normally between 550 and 650°C for steel parts. Soaking time is about one to two hours. After the soaking time the components should be cooled down slowly in the furnace or in air. A slow cooling speed is important to avoid tensions caused by temperature differences in the material, this is especially important when stress relieving larger components.

Due to configuration of the available furnace, rail specimen was cut till the length of 1800mm. Considering that the length between the supports is 1200mm this modification should not affect the results of the experiment.

4.2 The test

4.2.1 Description of the test

The flexural behaviour of the rail 60E1 under purely vertical load is investigated. The research work involves a so-called four-point bending test. The goal of the experiment is to reach bending capacity of the beam until plastic behaviour of the rail specimens is obvious.

The tests were conducted with loading controlled by displacement. Displacement control rate was set 0.05 mm/s.

Two independent tests were conducted:

1. Four-point bending test of "as fabricated" 60E1 railway rail (2000mm sample)
2. Four-point bending test of the heat-treated 60E1 railway rail (1800mm sample)

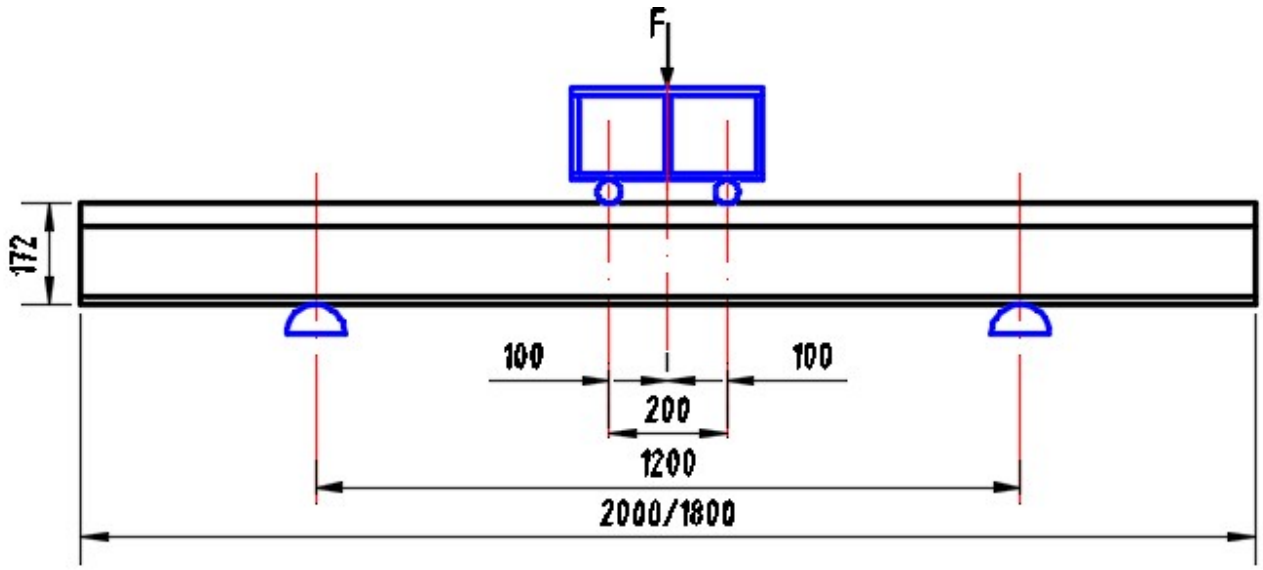

Figure 12. Layout of four-point bending test

4.2.2 Test samples

The laboratory test sample is a 2m (1.8m) piece of railway rail 60E1 also known as UIC60. For the needs of the bending tests, two rail pieces 2m long each were purchased from Strabag rail. Detailed drawing is presented in Annex 1. Quality Certification protocol for delivered rails is presented in Annex 2.

4.2.3 Preparation for the test

4.2.3.1 Load-application mechanism (Arrangement for Loading)

The test specimen has been arranged for undergoing vertical loading. Vertical load has to be applied on two points. FE model of the experiment was prepared previous to testing specimens (see Part 6 of current thesis). As a result of preliminary FEM simulation, plastification of the rail due to bending is expected on the maximum level of 1200 kN. Therefore the main demand for load-application structure is to withstand applied load and not to break before plastification of the rail is reached. Load-application structure is made of HEB160 section with 12mm thick end plates and 12mm thick intermediate stiffener. Considering that the rail is curved on top, additional stabilization is provided by means of plates overlapping the rail and fixed with bolts.

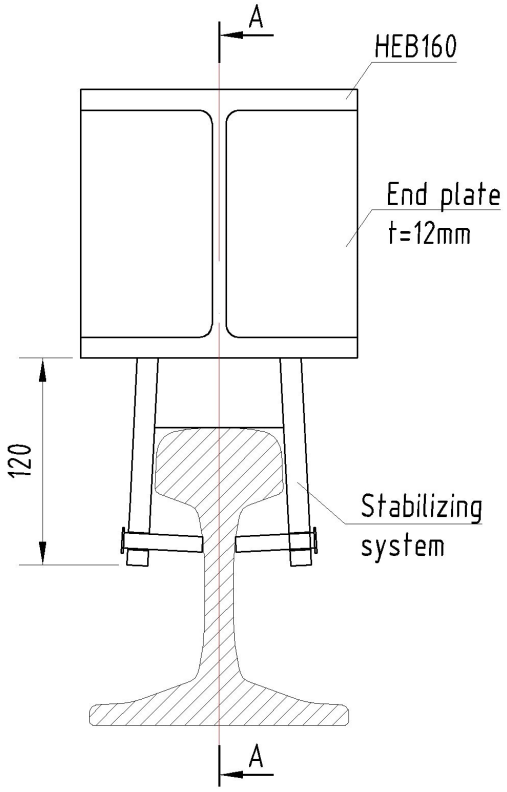

Figure 13. Load-application structure. Dimensions. Front view

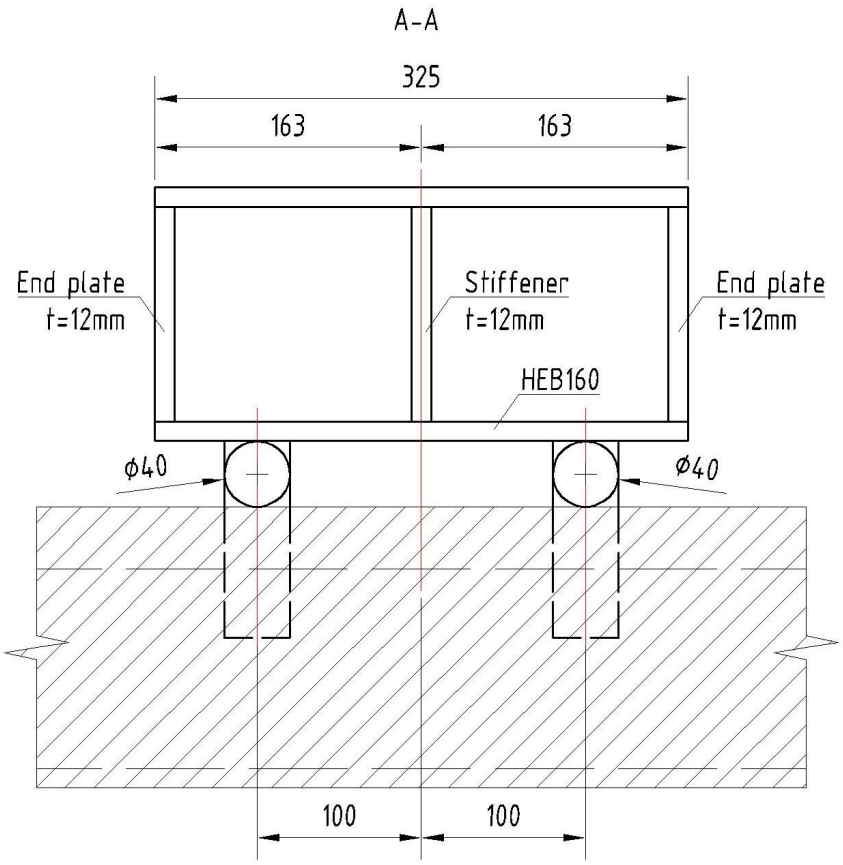

Figure 14. Load-application structure. Dimensions. Cut A-A

Figure 15. Load-application structure. Photo

4.2.3.2 Position of sensors

Two main types of sensors are attached to the specimen in the current test:

1. Displacement sensor
2. Strain gage

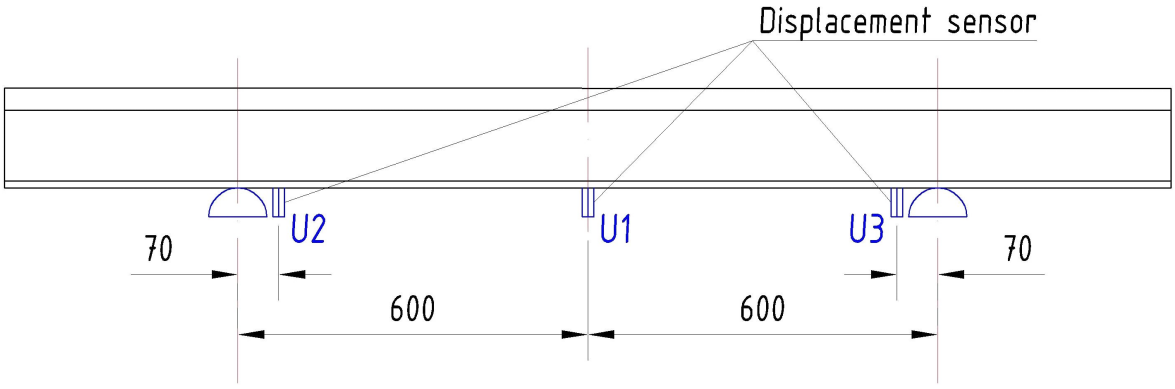

Figure 16. Positioning of displacement sensors

Displacement sensors are potentiometr sensors and they have a range from 0 to 100 mm. Sensors near support are installed for capturing instabilities of any nature that can occur during the test.

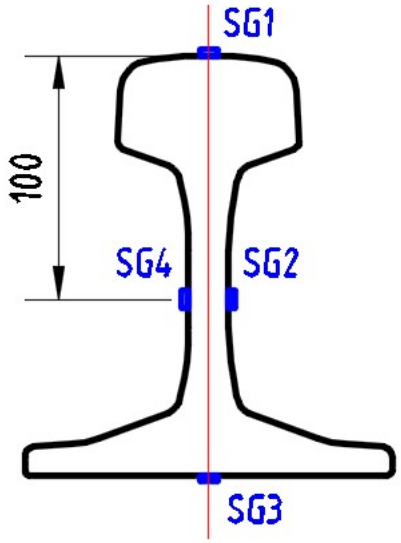

Figure 17. Position of strain gages

High strains are expected at the top and bottom, so strain gage for high strains should be applied there. Strain gages on the web are placed symmetrically on both sides in order to capture instability of the web if it will occur.

Table 2. Strain gauges used in the test.

Strain gauge	Max elong. [μm/m]	Resistance [Ω]	Gage factor	Length [mm]	Assignment
1-LY11-6/120	±20,000	120±0.50%	1.99±1.0%	6	SG2, SG4
1-LD20-6/120	±100,000	120±0.50%	1.99±1.5%	6	SG1, SG3

4.2.4 Test report. Analysis of test output data

4.2.4.1 Loading history analysis

4.2.4.1.1 Load-displacement curve

The load applied to the specimen has been plotted against the vertical displacement of the Centre Point (Um). Settlement of the rail on its supports Uc, which includes local crashing of the material of supports, leads to additional vertical displacement captured by U1. Uc should be subtracted from total vertical displacement U1 of the Centre point. Uc was assessed by means of rotation of the rail near supports, performed calculations can be found in Annex 3.

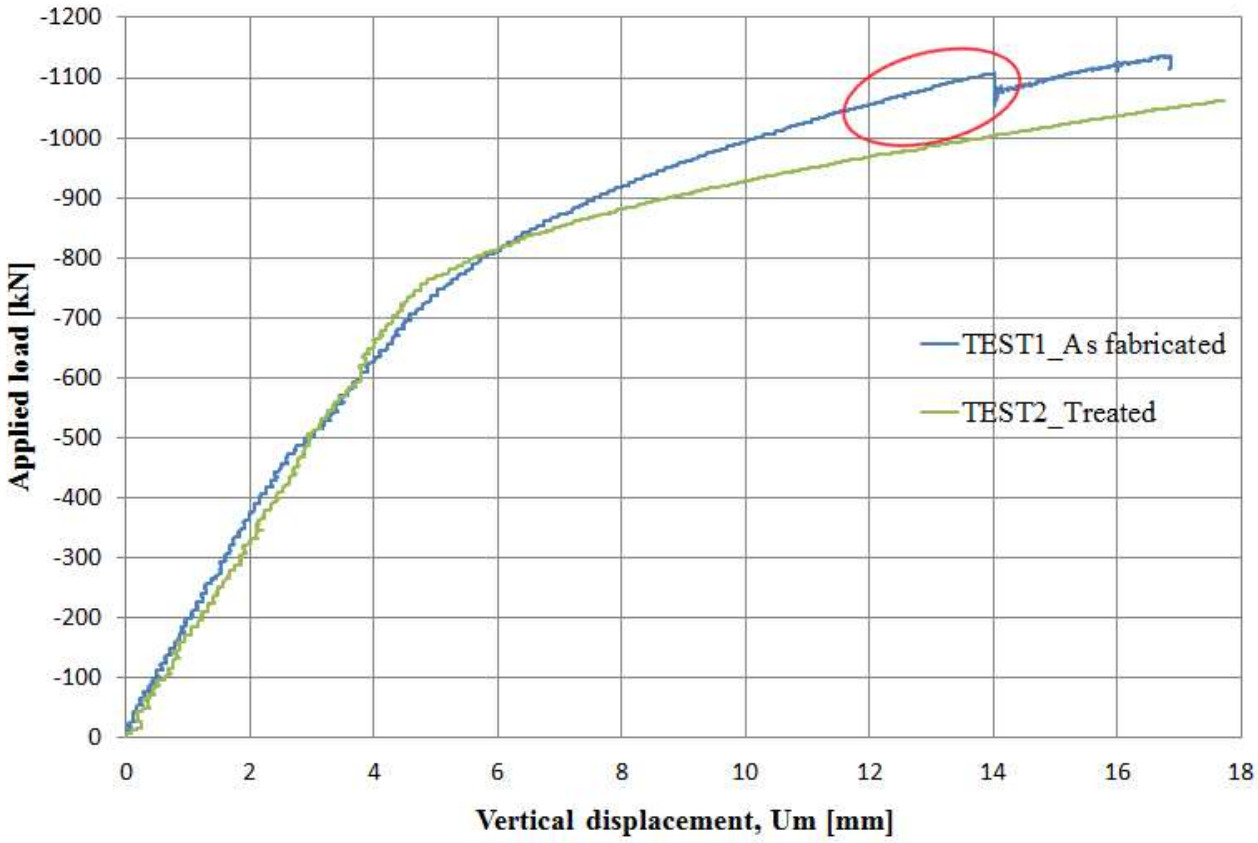

Figure 18. Applied load vs Um

Inhomogeneity on a part of curve for “as fabricated” rail can be observed (circled with red). That is a result of buckling of a lower flange of load-application structure.

Figure 19. Buckling of load-application structure.

It can be seen from Figure 14 that the linear portion of curves are consistent, while the actual variations are in the initiation and the trend in the inelastic part. Since rail steel is a ductile material and exhibit elastic-plastic behaviour, plastic bending occurs when an applied moment causes the outside fibres of a cross-section to exceed the material's yield strength. As the bending stress is not uniform over the section, there is no sudden drop of the load. When outer fibres become plastic the load start dropping but gradually, so there is no sharp point which it is possible identify.

4.2.4.1.2 Experimental Load-Strain curves

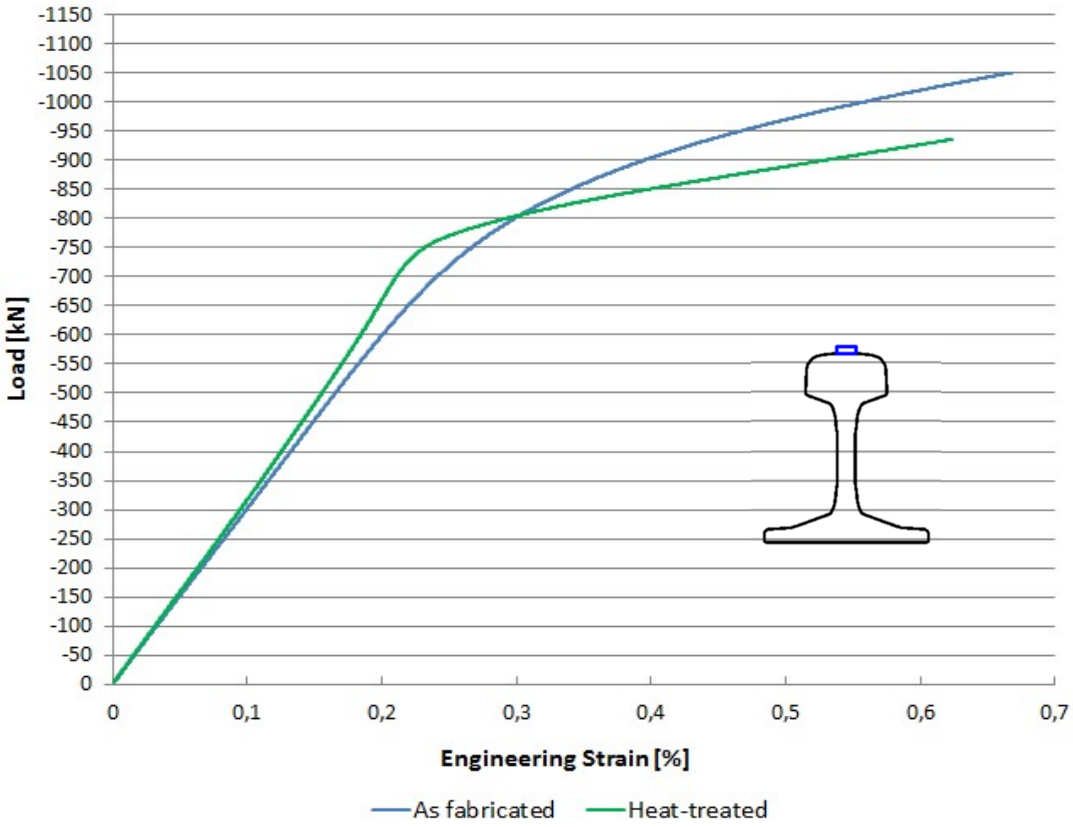

Figure 20. Load-strain curve for top center-point

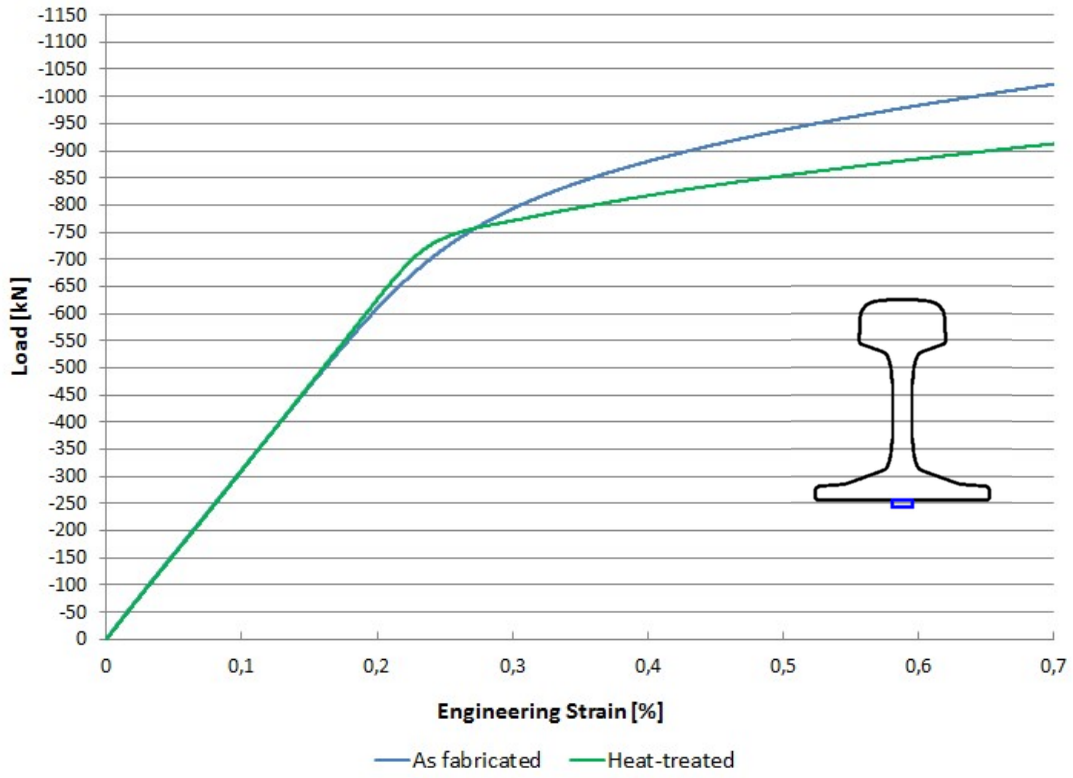

Figure 21. Load-strain curve for bottom center-point

Since load-strain curve is similar to the stress-strain curve of the material it is made of, then it is possible to conclude that material properties are different for specimens. As they were supplied by the one manufacturer then the rail were more likely affected by heat-treatment.

Heat-treatment process that was conducted. Temperature of heat-treatment varied between 550 and 650°C. In the same time with stress releasing annealing could occur.

Annealing, in metallurgy and materials science, is a heat treatment that alters the physical and sometimes chemical properties of a material to increase its ductility and reduce its hardness, making it more workable. Hardness is an engineering property and it has strong usefulness in characterization of different types of microstructures in metals and is frequently used in the context of comparing things like tempered metals. There are no apparent changes in elastic modulus in metals that have undergone different hardening treatments so the hardness is a good indication of the underlying microstructure.

Therefore it was decided to investigate and compare properties of steel for “as fabricated” and heat-treated rails.

4.2.4.1.3 Hardness test

Hardness tester KT-C NDT1 KRAFT is used for hardness determination. It is a hand-held Rockwell hardness tester, indentation hardness of the material is measured. It is based on a fact that yield strength and tensile strength were found to have a linear correlation with hardness for steels with yield strengths of 325 MPa to over 1700 MPa and tensile strengths between 450 and 2350 MPa [13]. Hardness tester KT-C NDT1 KRAFT provides us with values of tensile strength directly from the device that need to be compared. Advantage of the hardness tester KT-C NDT1 KRAFT is that measurements can be easily done ‘in the field’ (Figure 22). Measurement was done at the distance of 40 cm from the middle point of the specimen. Hence zone where plastification due to bending occurred is avoided. Results of testing are presented in the following table.

Table 3. HB hardness measured by hardness tester KT-C NDT1 KRAFT

Position	HB hardness, "As fabricated" rail	HB hardness, Heat-treated rail	Difference, [%]
Top	231	201	14
Web	228	197	15
Foot middle	235	208	12

Table 4. Tensile strength measured by hardness tester KT-C NDT1 KRAFT

Position	Tensile strength, "As fabricated" rail, [MPa]	Tensile strength, Heat-treated rail, [MPa]
Top	748	706
Web	739	675
Foot middle	784	700

There is a fairly large difference between obtained values. Heat-treated rail specimen has lower values of hardness and therefore tensile strength.

Figure 22. "Field" test. Hardness measurement

4.2.4.1.4 Reason behind deviation

Results of the hardness measurement gives us a reason to conclude that heat-treatment process indeed changed material properties that affected flexural behaviour of the rail in inelastic range.

As we can't trustworthy compare plastic behaviour of both specimens due to difference in material properties, stress distribution in cross-section in elastic range might be compared. Test specimens respond elastically to the applied load until displacement of the centre point reaches the certain value. According to Figure 18, linear, elastic part of graph is consistent until displacement Um of 4 mm.

4.2.4.2 Stress-distribution in central cross-section

Experimental data is given as an absolute value of strain in the point of application. Consequently corresponding stress is calculated in accordance with:

$$\sigma = \varepsilon * E$$

Where, ε – value of strain,

E – Young's modulus (E=210GPa).

Stresses corresponding to displacement Um of 4 mm are presented in the following table:

Table 5. Values of stresses in central cross-section (displ. 4mm). Experimental data

"As fabricated"	**Strain [um/m]**		**Stress [MPa]**
Top	-2101		-441,2
Web	197	129	34,2
Bottom	2067		434,1

Heat-treated	**Strain [um/m]**		**Stress [MPa]**
Top	-2008		-421,7
Web	11	70	8,5
Bottom	2124		446,0

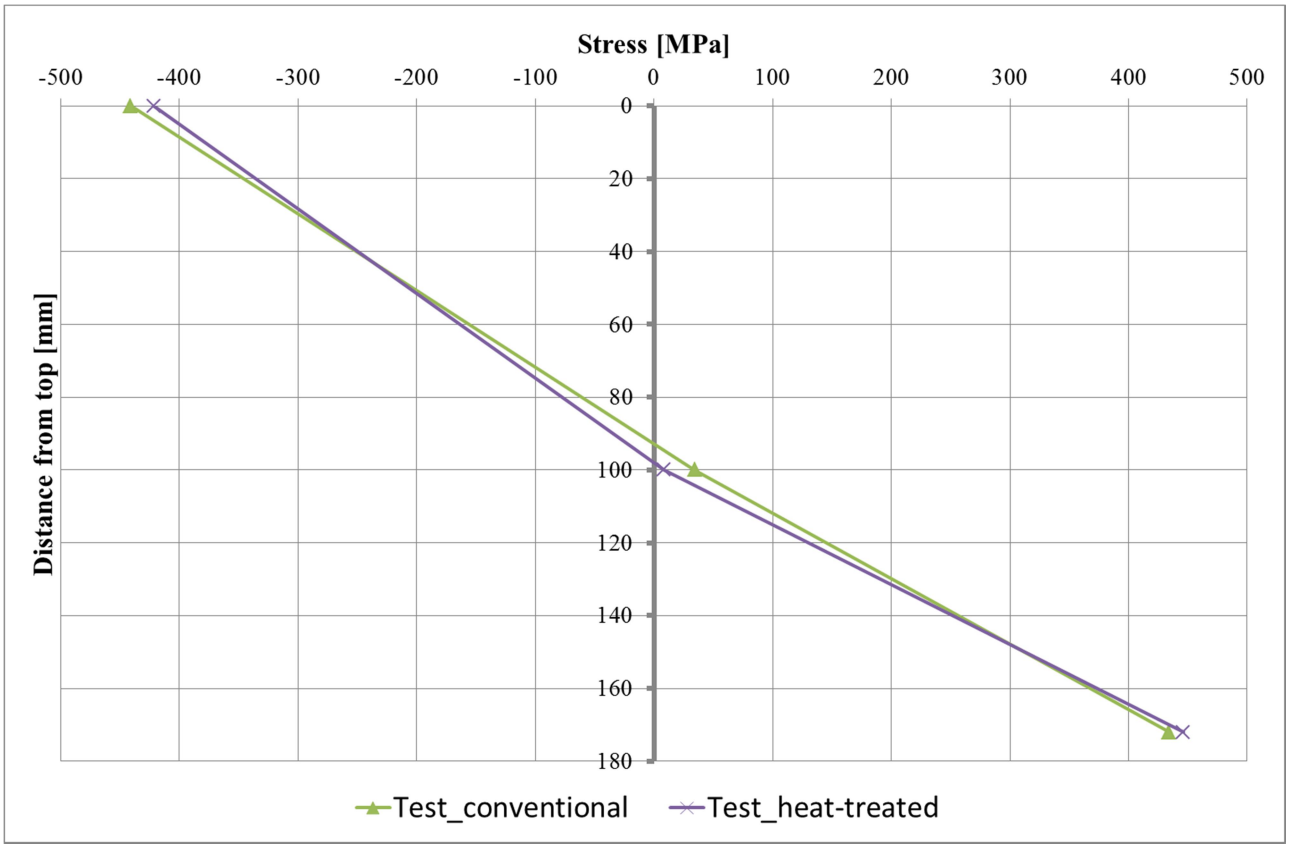

Figure 23. Distribution of stresses in central cross-section (displacement 4mm)

4.2.4.2.1 Analytical solution for stress distribution

The stress distribution due to the flexural behaviour was as well analysed in accordance with conventional prismatic beam theory:

$$\sigma := \frac{M \cdot z}{I}$$

where:

- z-distance from point under consideration to neutral axis
- I-moment of inertia
- M-bending moment

Bending moment for the case of four-point bending is therefore:

$$M := \frac{F \cdot (L - l)}{4}$$

where:

- F-force applied

- L-distance between the supports
- l-distance between points of load application

Calculated stress values are presented in the table below:

Table 6. Values of stresses in central cross-section. Analytical solution

	Stress [Mpa]
Top	-487
Foot	433

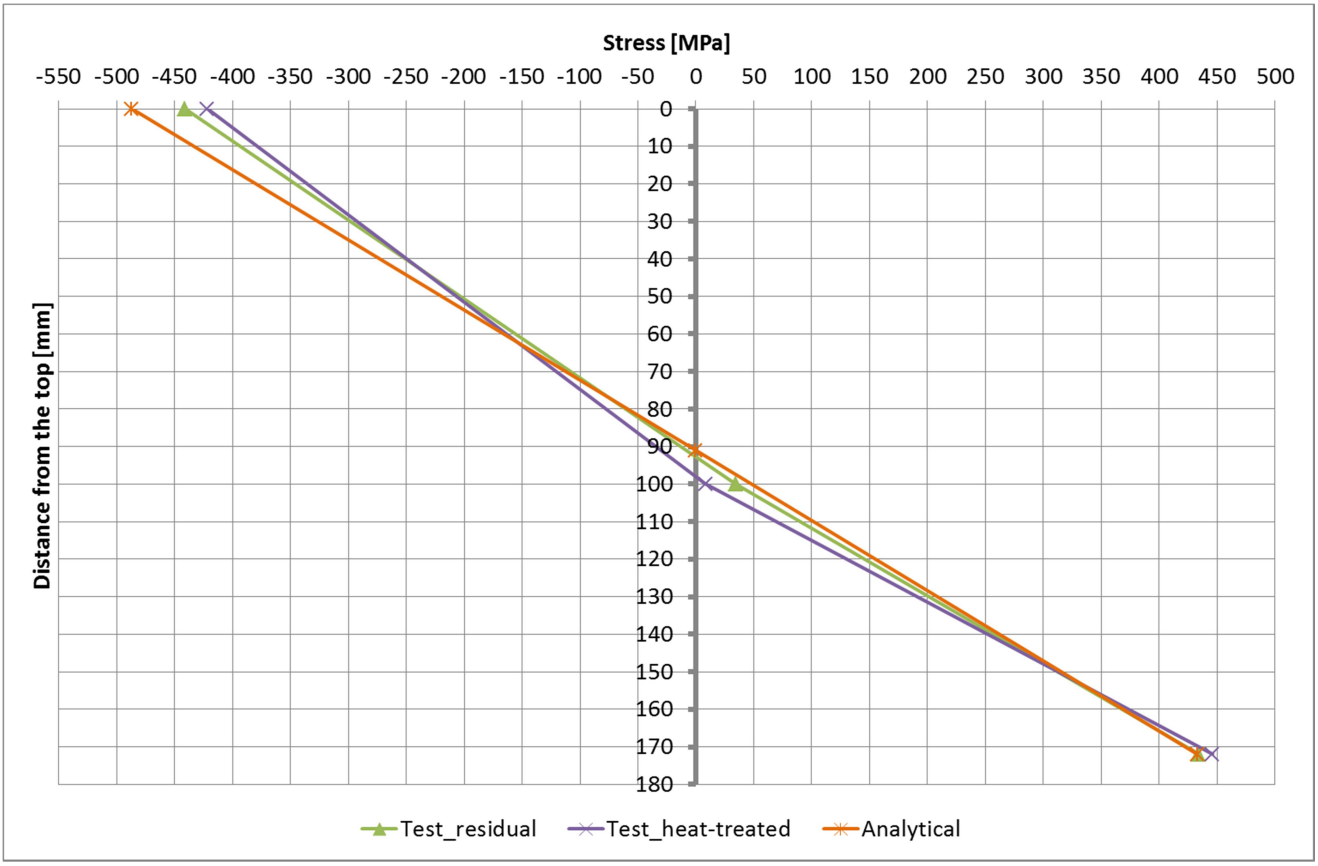

Figure 24. Distribution of stresses in central cross-section. Comparison: Test vs. Analytical

Experimental data and calculated stress values show good agreement, although some deviation was expected due to the alignment of specimen in the bending setup.

5 RESIDUAL STRESS MEASUREMENT

5.1.1 Description of the test

In order to find the value of residual stress in the rail foot experiment was done. The test piece was taken from the same heat as the test pieces for the four-point bending tests. The value obtained shall be compared with the one defined by EN 13674-1:2011.

Rail foot surface longitudinal residual stress shall be found according to EN 13674-1:2011 Annex C. Procedure proposed by European Committee for Standardization (CEN) is a destructive technique. The surface to which the gage is attached shall be progressively isolated from the rail. Then relaxed strains shall be used to estimate the stresses that have been relieved whilst the original residual stresses are taken to be those values but with a change of sign. In other words, two saw cuts shall be made to remove 20mm thick slice, released strains should be measured.

5.1.2 Preparation of the test

Test piece is 1 m long rail (acc. to 8.5.2, EN 13674-1:2011). It was taken from the same heat as specimens prepared for the four-point bending.

The strain gauge shall be attached to the surface of the rail foot in order to measure longitudinal strain at the positions as shown in picture below (Figure 25).

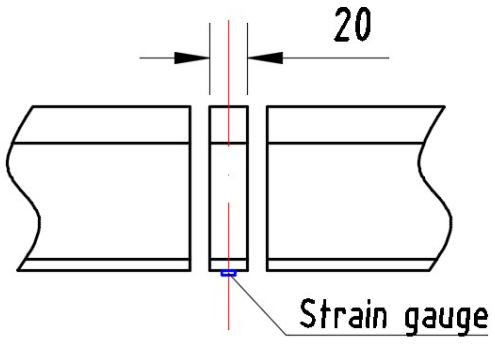

Figure 25. Position of strain gauge

Two strain gauges were used in order to increase the safety of measurements. 1-LV41-3/120V satisfies the requirements of C.2 Annex C. 1-LV41-3/120V was attached in the

middle of the foot, additional strain gauge 1-LY11-1.5/120 on the distance of 10 mm from it. The latter was used in order to increase reliability of results.

Table 7. Strain gauges used in the test.

Strain gauge	Encapsulation	Resistance [Ω]	Gage factor	Length [mm]
1-LV41-3/120V	Yes	120±0.50%	1.99±1.0%	3
1-LY11-1.5/120	No	120±0.35%	1.99±1.5%	1.5

1-LV41-3/120V 1-LY11-1.5/120

Figure 26. Strain gauges used

The surface of the rail foot shall be prepared and the strain gauge shall be attached. Any surface preparation shall not result in a change of the residual stresses in the rail foot.

First, rust was removed by polishing.

Figure 27. Preparation, first step

Second, strain gauges were glued to the rail by two component glue HBM X60 and then covered with a silicon adhesive for the water protection.

Figure 28. Preparation, second step

5.1.3 Test report

While cooling the rail to maintain a constant temperature, two saw cuts were made to remove a 20 mm thick slice from the center of the rail length. “Pilous” band saw with automated water cooling was used.

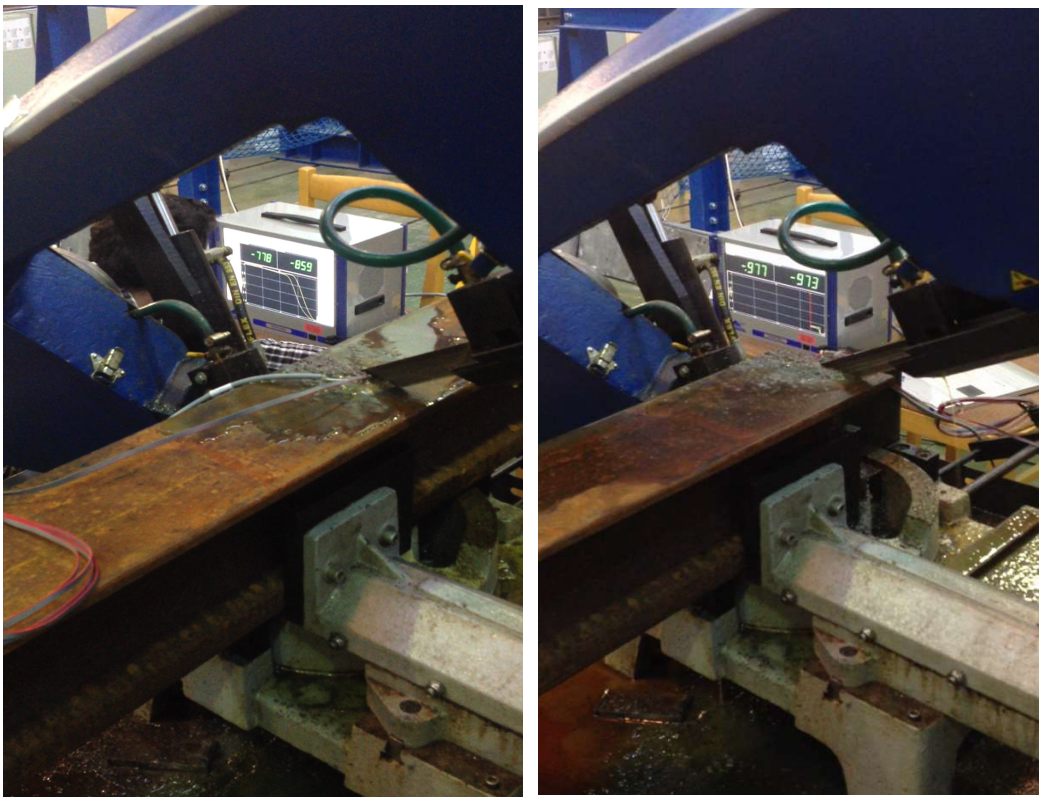

Figure 29. Test process.

The strains released during the cutting process were measured (Figure 30).

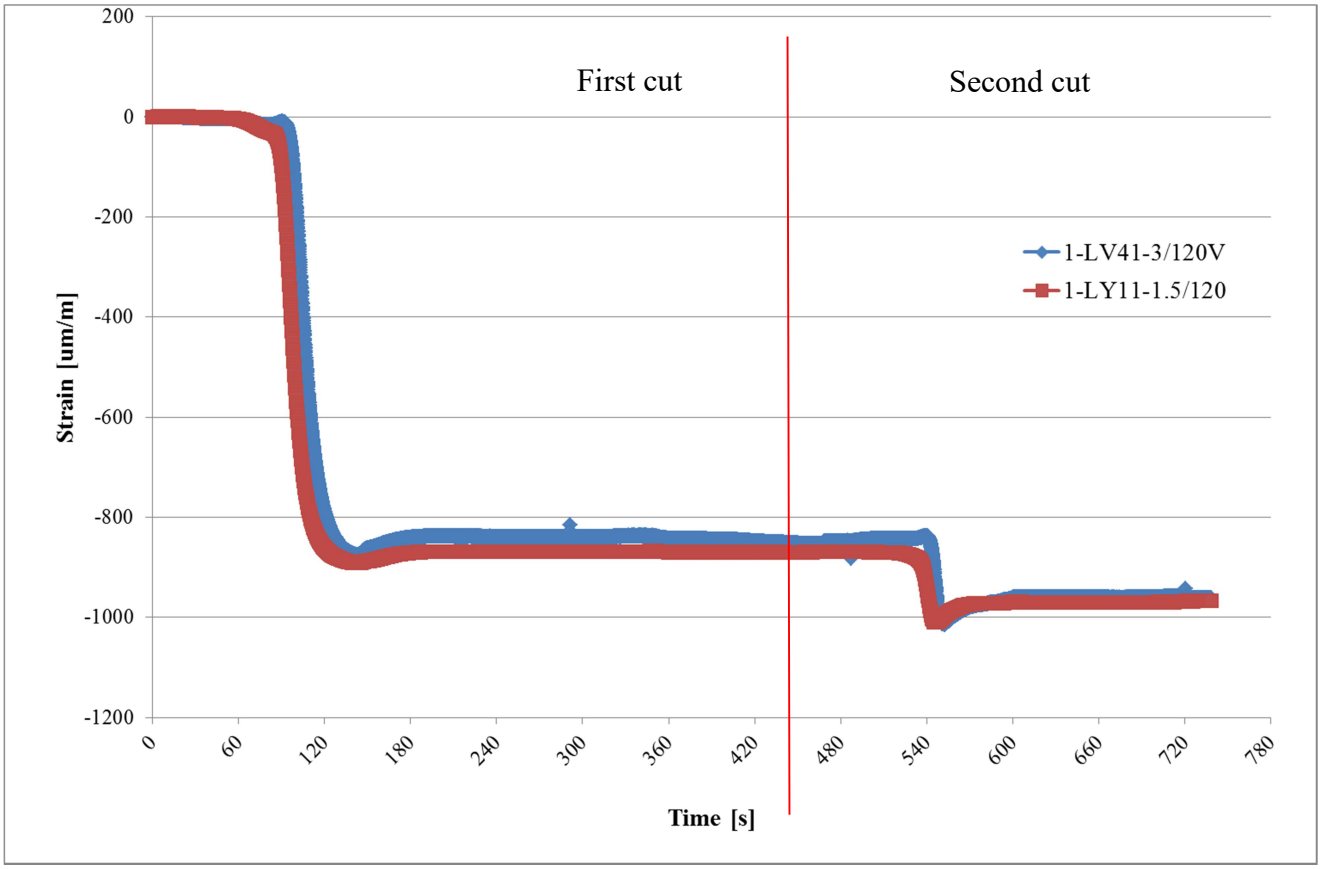

Figure 30. Strain measurement

Good agreement can be observed between values measured by two strain gauges.

Final values of strain are:

1-LV41-3/120V: -962 um/m

1-LY11-1.5/120: -967 um/m

The difference between measured final strains is less than 1%.

The highest strain developed relates to the first cut. That means that highest stress was released after first cut.

In the ends of each slope we can see two peaks that are related to the moment when saw was passing the sensors. Thermal expansion of the steel due to friction might take place, even though saw was constantly cooled. After some time temperature returns to lower values and so strains do.

Residual stress in the rail foot can be calculated using the Young Modulus 210 GPa. Value of strain taken from 1-LV41-3/120V I used:

$$962\,um/m \times 2.01 \times 10^5\,MPa = 202\,MPa$$

Measured value is below the limit of 250MPa defined by EN 13674-1:2011.

6 NUMERICAL MODELLING

Abaqus/CAE 6.14 is used for finite element modelling. Feature-based, parametric modelling makes Abaqus/CAE a highly efficient and effective pre- and postprocessor for every analysis need.

6.1 Basic principles of modelling

6.1.1 Types of elements

Abaqus/CAE provides a wide range of elements for different geometries and analysis types.

Each element can be characterized by considering the following:

1. Family (Continuum, shell, membrane, rigid, beam, truss elements)

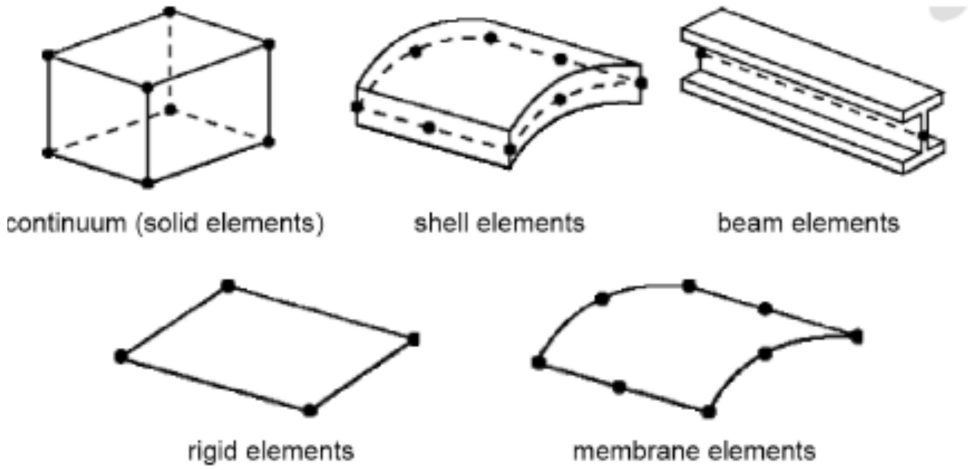

Figure 31. Main types of elements

2. Number of nodes

An element's number of nodes determines how the nodal degrees of freedom will be interpolated over the domain of the element (Figure 32).

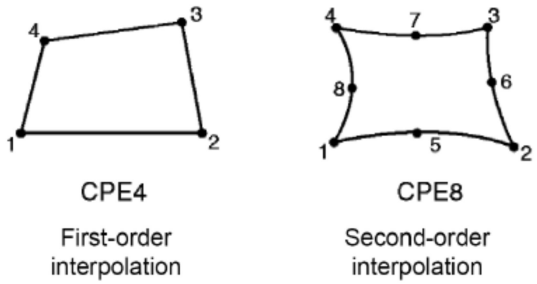

Figure 32. Interpolation types

3. Degrees of freedom (Displacements, rotations, temperature)
4. Formulation (Plane strain, small-strain shells, plane stress, finite-strain shells, hybrid elements)
5. Integration

The stiffness and mass of an element are calculated numerically at sampling points called "integration points" within the element. The numerical algorithm used to integrate these variables influences how an element behaves.

Table 8. Integration types

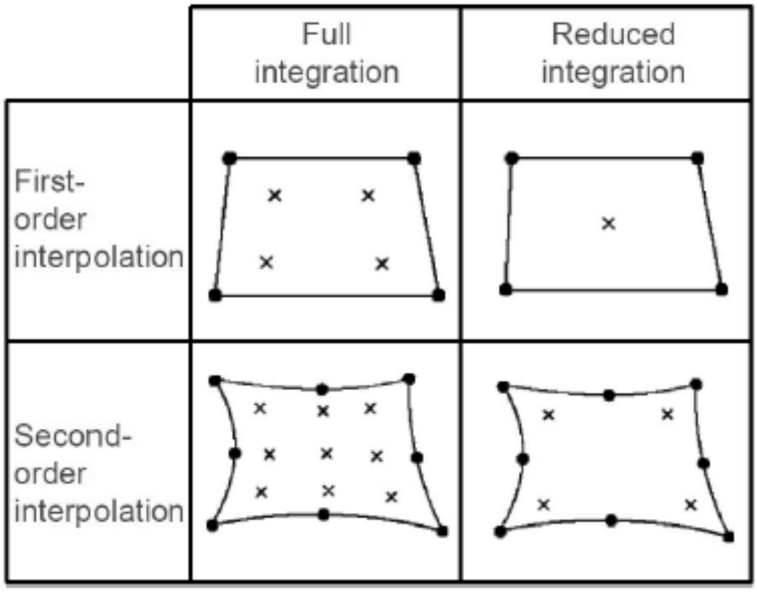

6.1.2 Modelling bending problems

According to the Abaqus user guide: "If the problem involves bending and large distortions, use a fine mesh of first-order, reduced-integration elements."

Reduced-order integration allows for fast and cheap calculation but the use of this integration algorithm comes with some drawbacks.

Hourglassing can be a problem with first-order, reduced-integration elements (CPS4R, CAX4R, C3D8R, etc.) in stress/displacement (bending) analyses. Since the elements have only one integration point, it is possible for them to distort in such a way that the strains calculated at the integration point are all zero, which, in turn, leads to uncontrolled distortion of the mesh.

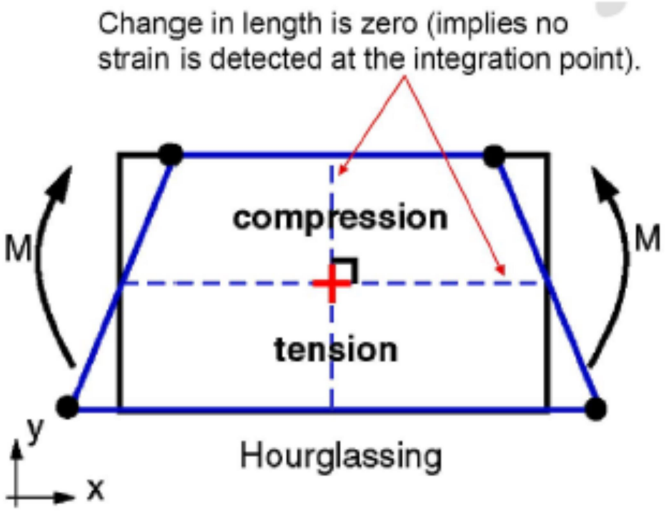

Figure 33. Bending behaviour for a single first-ordered reduced integration element

First-order, reduced-integration elements in Abaqus include hourglass control, but they should be used with reasonably fine meshes. Hourglassing can also be minimized by distributing point loads and boundary conditions over a number of adjacent nodes or by the usage of load-application bodies.

Hourglassing can usually be seen in deformed shape plots. It can be seen on Figure 34 where different mesh density was applied.

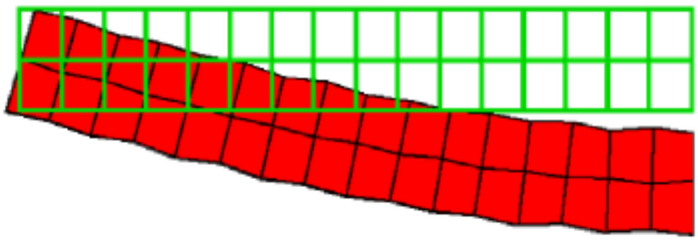

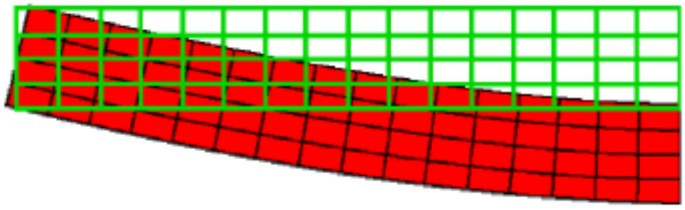

Figure 34. Cantilever in bending

6.1.3 Mesh generation

Meshing of the element with appropriate density and element type allows balancing computational resources and precision of analysis. Elements are generated in the Mesh module of Abaqus/CAE. For three-dimensional continuum (solid) bodies hexahedral and tetrahedral elements can be used.

A)

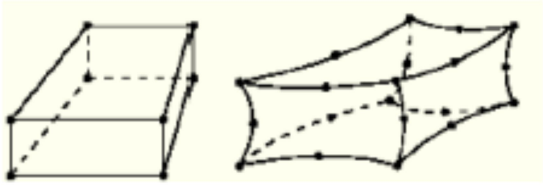

B)

Figure 35. Reduced and fully integrated hex (A) and tet (B) elements

Abaqus user guide recommends “Application of quads and hex elements are generally recommended whenever possible however these elements are geometrically less versatile and difficult to be used for complicated geometries.”

Special attention should be paid to tetrahedral meshing. Even though tetrahedral elements provide geometrically versatility they are overly stiff, especially for bending problems, and are not recommended for the use in structural analysis.

Considering possible problems that can appear due to bending (6.1.2) and meshing of the complex geometry, mesh convergence study should be done. The problem should be simulated using progressively finer meshes. When two meshes yield nearly identical results, the results are said to have “converged.”

6.2 Development of numerical model

Four-point bending test is modelled in Abaqus/CAE. It is possible to simulate all the aspects of the real experiment including support conditions and load application structure.

Abaqus/CAE has no units built into it except for rotation and angle measures. Therefore, the units chosen must be self-consistent, which means that derived units of the chosen system can be expressed in terms of the fundamental units without conversion factors.

The International System of units (SI) is an example of a self-consistent set of units.

Table 9. Example of units in SI system

Quantity	SI	SI (mm)
Length	m	mm
Force	N	N
Time	s	s
Stress	Pa (N/m^2)	MPa (N/mm^2)

SI (mm) system is chosen for the current model.

6.2.1 Geometric modelling

Parts are the building blocks of an Abaqus/CAE model. Part module is used to create each part, and Assembly module is used to assemble instances of the parts.

1 Rail

Railway rail is modelled as a three-dimensional solid extrusive of predefined sketch of rail geometry. Solid element is very costly in terms of computational resources. Therefore only half of the rail along its length was modelled. Axis of symmetry is a line goes from the middle of the top to the bottom of the rail.

2 Supports and load pins

Supports and load pins are modelled as a solid semi cylinder. Beam is extended beyond the support so that it won’t leave the support due to rotations.

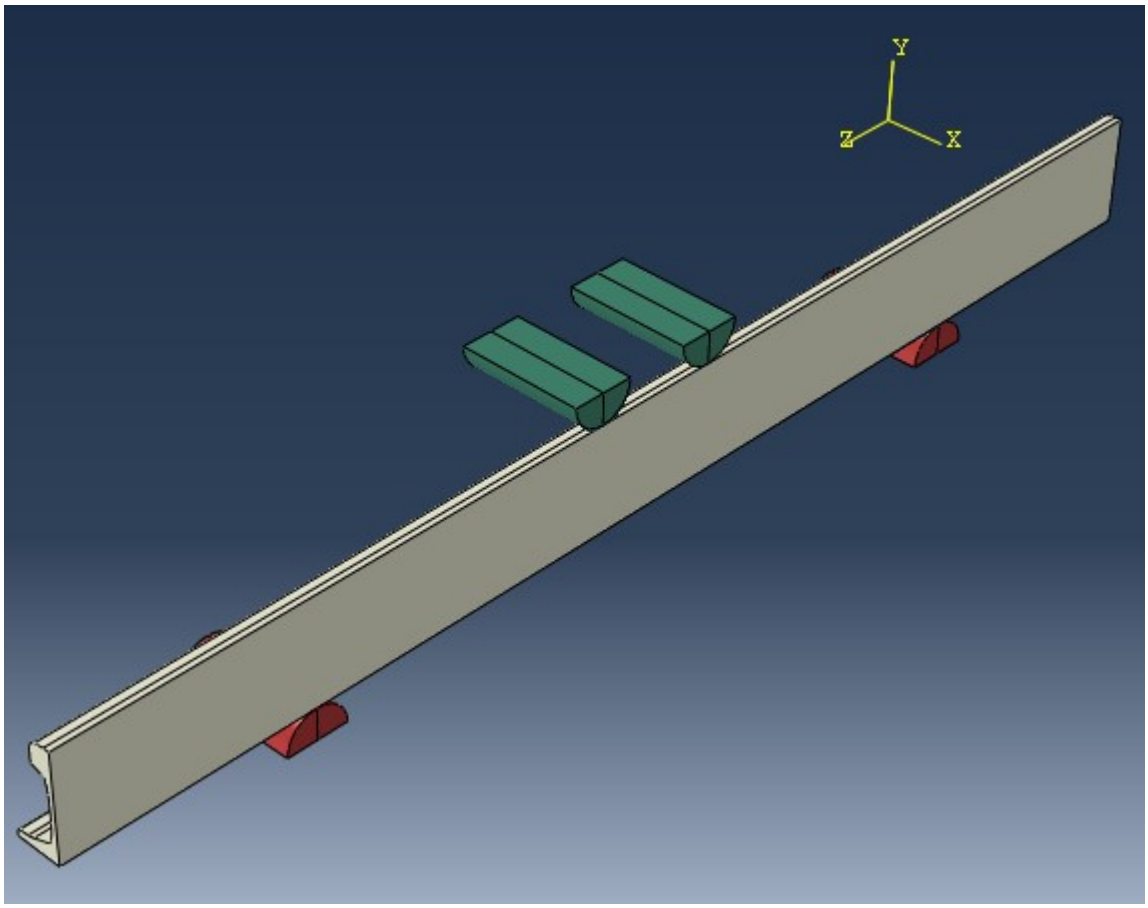

Figure 36. Final assembly

6.2.2 Boundary conditions and interaction

1 Boundary conditions

For simplification, only half of the model is simulated. In that case boundary conditions should be applied on the mid-plane of the rail and sides of supports and load pins. Movement in the direction perpendicular to longitudinal axis are restricted (displacement in X direction - Figure 36).

2 Interaction

The modelling of the four point bending setup in Abaqus/CAE come with some difficulties, since contact conditions are required and friction could not be omitted. Contact problem include severe non-linearities and requires additional computational resources. There are two contact pairs that should be defined: rail head and load-application structure; rail foot and support. Since rail head is curved and contact length is small comparing to one for the pair “rail foot and support”, frictionless property is used to define contact between rail-head and loading structure. Friction coefficient 0.5 (for steel-steel contact, dry and clean surfaces) is applied to define contact between rail-foot and support.

6.2.3 Load-application

The loading mechanism is modelled just above the beam and tied to a reference point. Loading in this case is a specified displacement that is applied to the reference point. By outputting reaction at the support the exact amount of applied load can be known. This modelling is exactly what the testing machine does.

6.2.4 Simulation of residual stresses

There are several options in Abaqus/CAE to define initial stresses:

1) Input of stress field from another job
2) User-defined initial stress field

As it was discussed in Part 2.2.3, output of FEM analysis is the residual stress field across the rail. However simulating of residual stresses' formation is not an easy task. All steps of production process should be carefully modelled. What is more, material model has to be able to account for cyclic plasticity including the hardening mechanisms. However once the numerical model is adjusted and validated with experimental data, precise residual stress field can be used in various other analyses including current study. Unfortunately there is no such model available for the open use for now. Therefore residual stresses are user-defined for the models in current work.

Initial stresses are defined using "predefined field" option in the Load module of Abaqus/CAE. Predefined field can be only applied to geometry (region). Therefore rail part requires comprehensive partitioning that replicates residual stress pattern.

Residual stresses in rail were characterized by various techniques described in 2.2.2.1-2.2.2.4 and simulated in 2.2.3. All approaches delivered the same stress profile with a typical 'C' shape and the maximal tensile stresses below the limit of 250MPa defined by the CEN standard. Although these approaches have their pros and cons. Advanced techniques like contour method and neutron diffraction method (2.2.2.2) provide us with a residual stress pattern with a relatively small step of measurements, however stress values on the surface are uncertain. Contrary, central hole-drilling which is a part of IC-DHD technique (2.2.2.4) is a well-known approach for measuring surface residual stresses.

Initial stress field should be applied to our model of UIC60 rail. No unified rail profile was used by researchers mentioned before (2.2.2, 2.2.3). Only simulation model provides us with the stress distribution for UIC60 rail. Weak point of this model is that it is considered to be close to real distribution, but still deviates from it. Thus it was decided to develop second

model with residual stress distribution based on contour method (2.2.2.3) as the most advanced for now in conjunction with IC-DHD (2.2.2.4). As the contour method was applied for different rail profile than UIC60, global idea of stress distribution was taken from this method and then the field was calibrated according to results of IC-DHD technique. IC-DHD technique was done for UIC60 rail profile.

Summarizing, two patterns of residual stresses in rail were adopted for current work:

1. RW-1: residual stress distribution according to numerical model (2.2.3) - Figure 37;
2. RW-2: residual stress distribution according to contour method combined with residual-stress data taken from IC-DHD technique (2.2.2.4) - Figure 38.

Maximum tensile residual stress in the foot was set to be equal to 202 MPa, according to the measurements that was done in the laboratory (5 - Residual stress measurement). Residual stress that we import to the model is always unbalanced, in other words, the system is initially in a non-equilibrium state. So we need to reach equilibrium before applying any loads or imposed displacements to our model. This can be done by defining an initial step without loads.

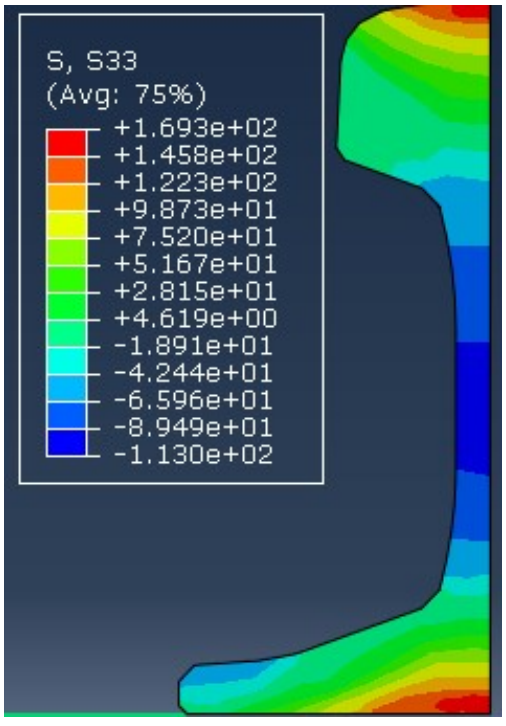

Figure 37. Residual stress distribution in RW-1

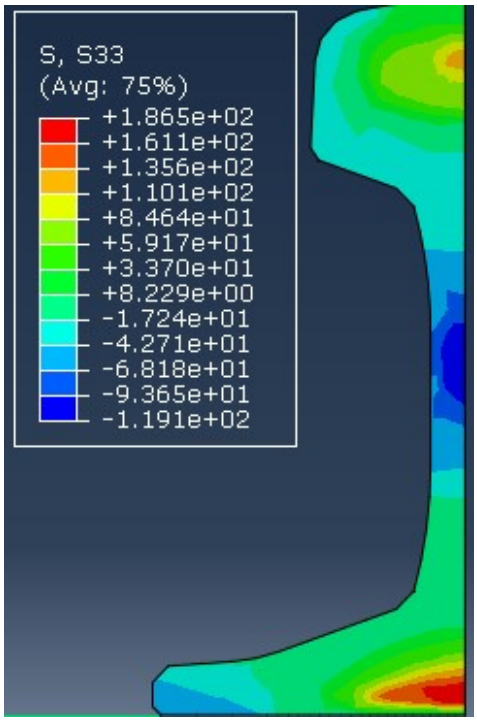

Figure 38. Residual stress distribution in RW-2

Longitudinal stresses in the middle cross section were obtained in the end of initial step when equilibrium of internal stresses was reached. For the sake of verification, introduced residual stresses shall be compared with stresses presented in 2.2.3 - Numerical modelling of residual stresses in rail and 2.2.2.4 - Incremental centre-deep hole drilling technique (IC-DHD).

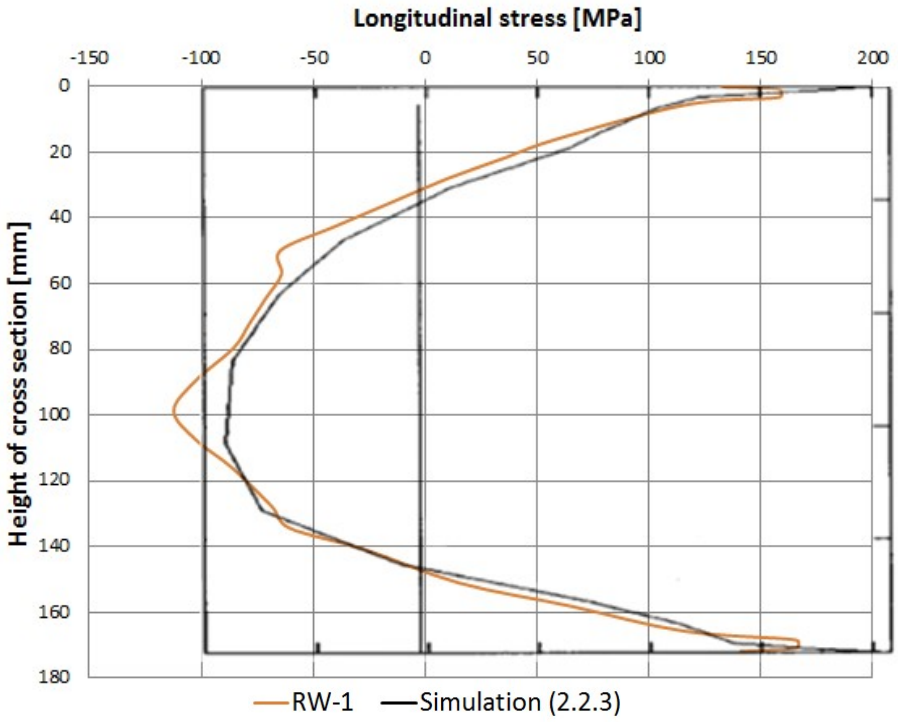

Figure 39. Residual stress verification. RW-1

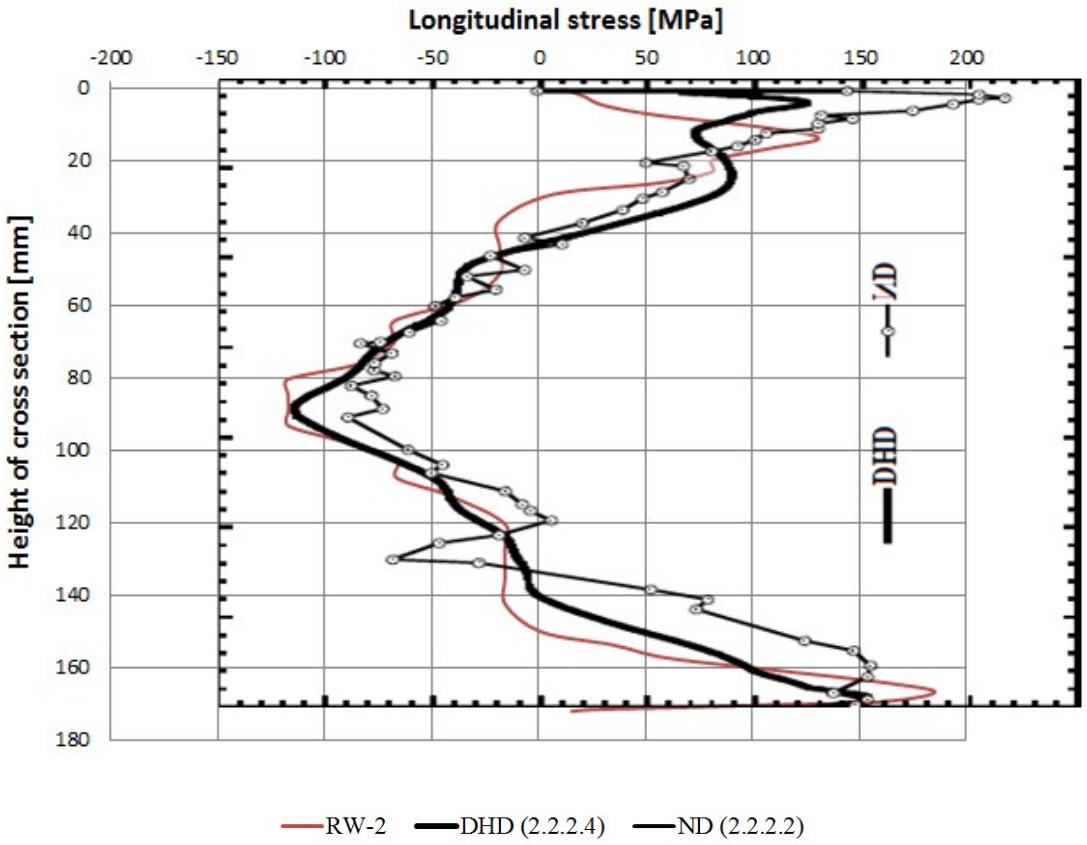

Figure 40. Residual stress verification. RW-2

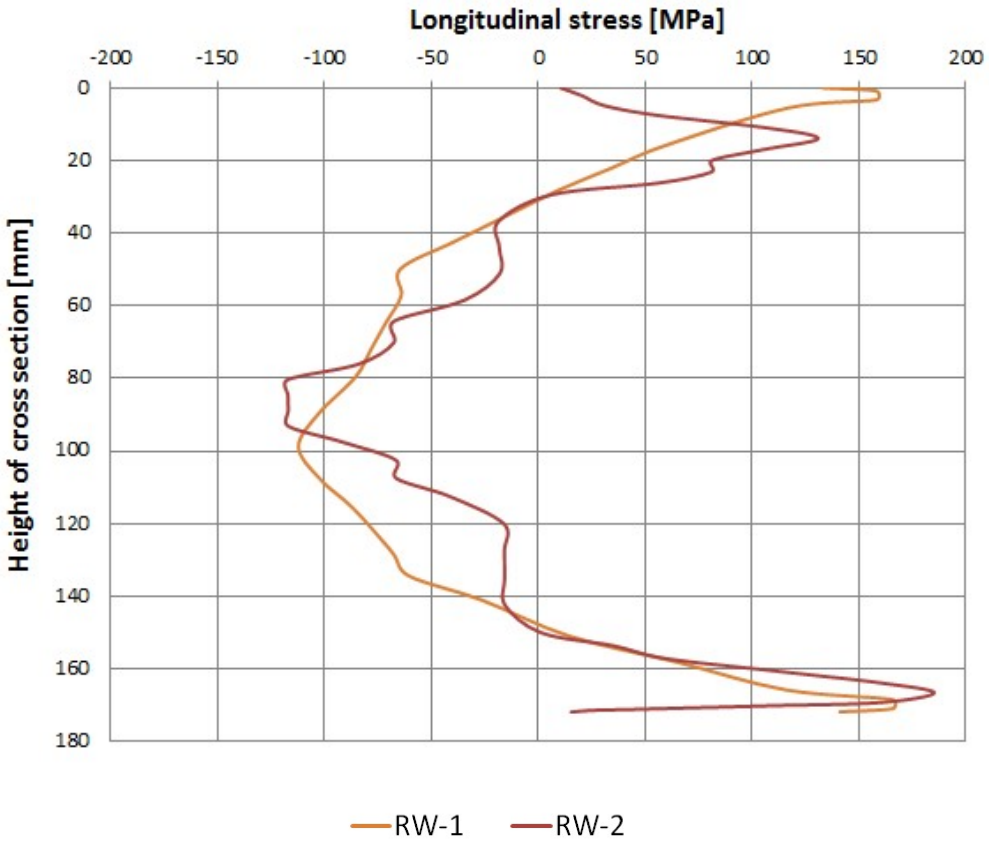

Figure 41. Residual stresses. RW-1 and RW-2

Residual stresses introduced in RW-1 and RW-2 show good agreement with residual stresses characterized in corresponding works. Though some scatter is observable. There is no flawless technique for measuring residual stresses, minimum intolerance is around 30 MPa for steels. Therefore existing scatter is considered acceptable.

Main difference between considering RW-1 and RW-2 is distribution of residual stresses near the surface. Now CEN standard controls maximum value of tensile residual stress in the rail foot. As we could see from the investigations presented in 2.2.2 and 2.2.3, position of maximum residual stress can differ for investigating approaches. Therefore two models with different initial stress distribution shall be studied.

6.2.5 Mesh generation

Simulating of residual stress with “Predefined field” tool requires comprehensive partitioning of the rail section. Edges of the each part have curved shape.

Mesh verification tool in Abaqus/CAE was used to find elements that could be extensively distorted due to their shape. If the one occurred, additional seed of the edge could be used, for instance.

Hexahedral mesh is needed to be fine in order to mesh those parts. 544 000 hexahedral elements were created and verified for our rail model. Both global and local seeds were used with seed size varied from 2 to 6. That number of elements can be considered as approximate minimum number of hexahedral elements needed to mesh the instance. Bigger seed size in some parts leads to appearance of analysis warnings in mesh verification tool.

Since the rail cross-section shape is complex and include curved edges, combined hex-dominated quadrilateral mesh (hex/tet) might be applied. 45 200 hexahedral and tetrahedral elements combined were created and verified for our rail model. Global seeds size is 8.

As we can see, combined meshing approach allowed to decrease number of created elements significantly (10 times!). Though we should be careful with tetrahedral elements in structural analysis, because they are overly stiff. Therefore for making sure that hybrid hex/tetr mesh gives appropriate results, mesh convergence study is better to be done. For that reason two models were created:

1. Model-Cp: extensively partitioned model due to the need of introduction of residual stress field (see previous part 6.2.4) that was meshed with hex/tet meshing;
2. Model- C: without partitioning that was meshed with fine hexahedral mesh.

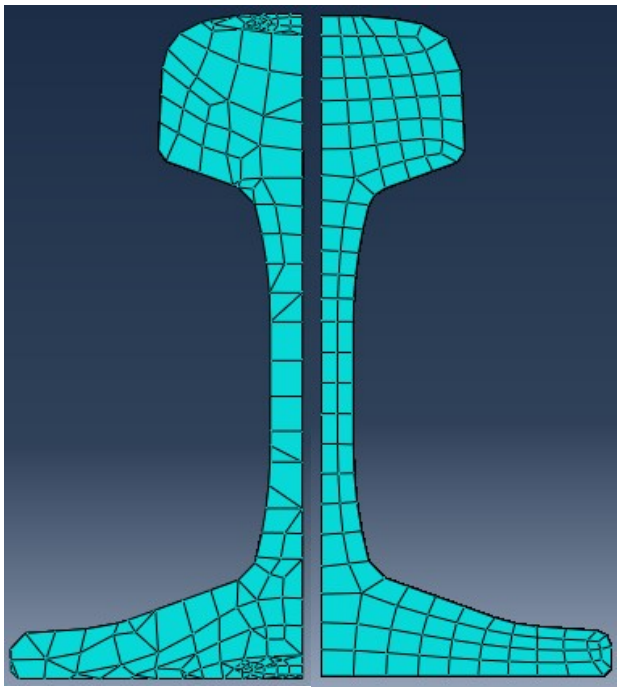

Figure 42. Meshing of the parts Model-Cp and Model-C

Four point bending simulation was conducted, bending load vs. displacement curves were compared.

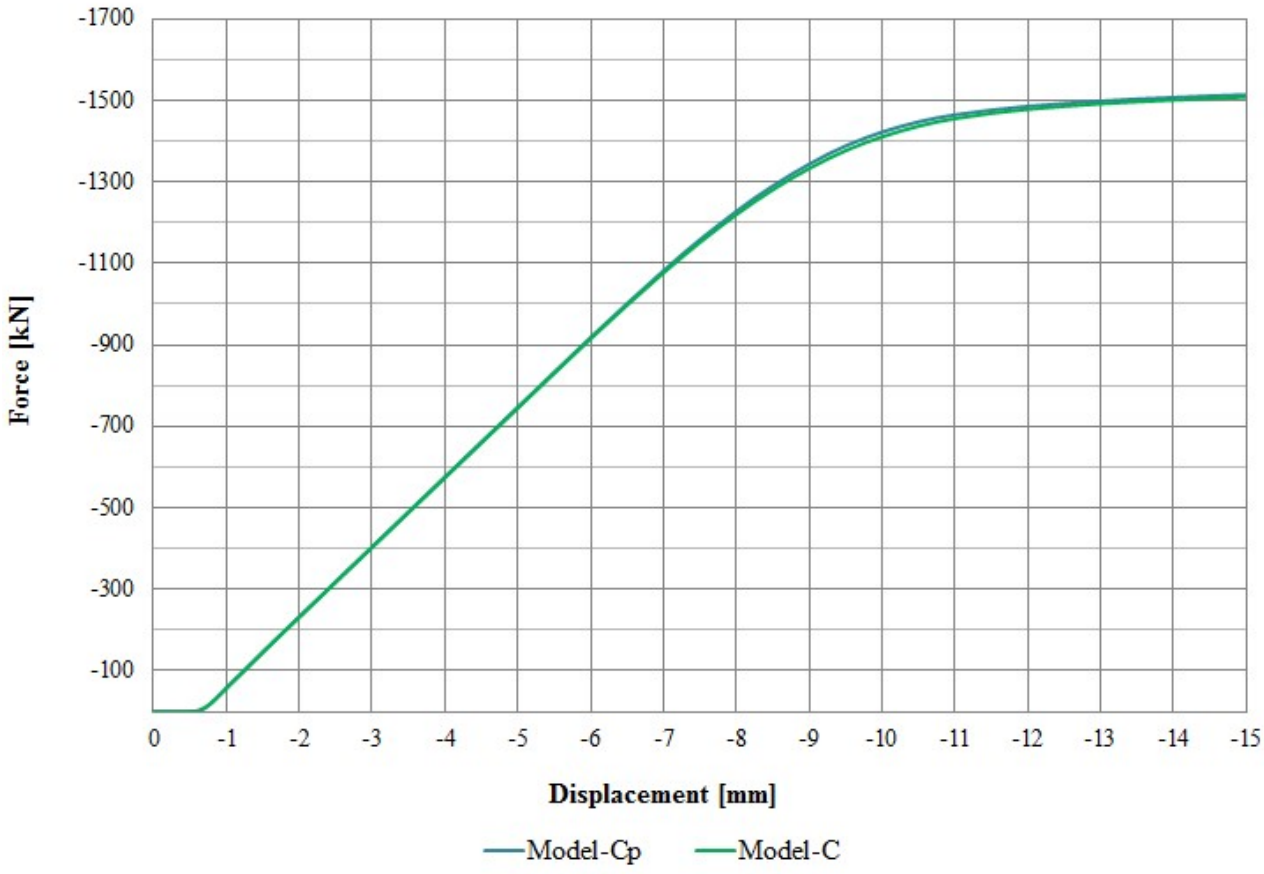

Figure 43. Mesh convergence study

As both plots show good agreement, hybrid hex/tet meshing was accepted for the model with introduced residual stresses.

6.2.6 Material model

Elastic modulus for S260 steel is 210 GPa, Poisson's ratio is 0,3.

In order to simulate plastic bending of the rail, plastic properties of S260 rail steel should be included in material model in Abaqus/CAE. Rail manufacturer could not provide stress-strain curve for S260 steel. Laboratory experiment could not be performed either. It was not possible to extract test samples from rail because of the limitation of the laboratory equipment. As a consequence of the absence of trustworthy material data, some deviations between experimental and numerical results are expected.

Plastic properties for S260 steel were found in following articles:

- TATA steel, Rail technical guide
- "Fatigue property analysis of rail steel based on damage mechanics"; Kengo Iwafuchi, Yukio Satoh, Yutaka Toi, Satoshi Hirose; Computational Solid Mechanics, Dept. Mechanical and Biofunctional Systems, Institute of Industrial Science, University of Tokyo
- Nonlinear analysis of residual stresses in a rail manufacturing process by FEM; C. Betegón Biempica,J.J. del Coz Díaz,P.J. García Nieto,I. Peñuelas Sánchez; Department of Construction and Engineering of Production, 33204 Gijón, Spain, Department of Mathematics, Faculty of Sciences, 33007 Oviedo, Spain

The hardening curve data are required in the tabular form of yield stress with plastic strain where the first pair of numbers must correspond to the initial yield stress at zero plastic strain.

Table 10. Plastic properties of S260 steel used in numerical model

Stress [MPa]	Strain
480	0
494	0.002
720	0.022
830	0.046
850	0.071

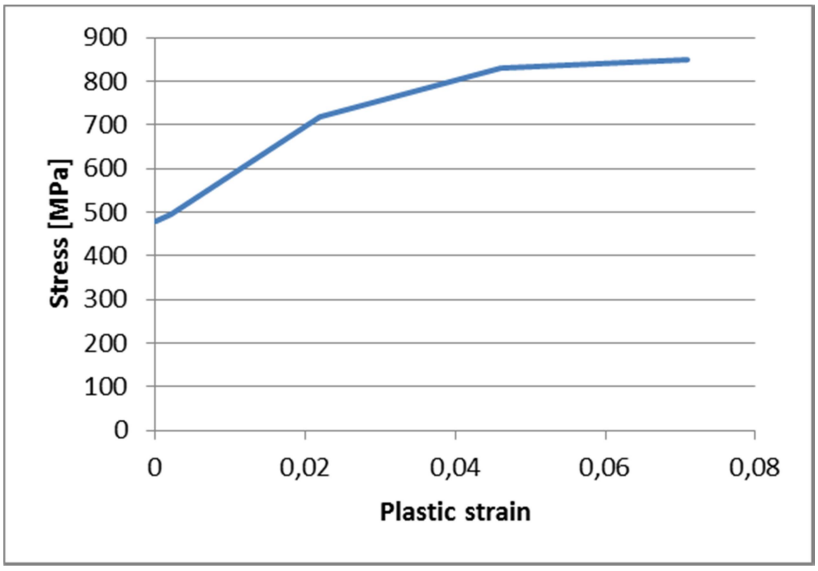

Figure 44. Yield stress vs. plastic strain. S260 steel

6.3 Validation of the model

Validation is the task of demonstrating that the model is a reasonable representation of the actual system: that it reproduces system behaviour with enough accuracy to satisfy analysis objectives. Experimental results shall be compared with numerical solutions.

First, global behaviour of the rail in bending is compared. It is represented as bending load vs. displacement of the middle point of the rail.

Following plots were compared:

1. Bending of "as fabricated" rail experimental data;
2. Bending of heat-treated rail experimental data;
3. Numerical RW-1. Residual stress pattern 1 (6.2.4);
4. Numerical RW-2. Residual stress pattern 2 (6.2.4);
5. Numerical RO-1 without incorporated residual stresses.

We expected to find some deviations between data from numerical and experimental data as a result of:

- Uncertain material model
- Alignment of the specimen in the bending setup
- Deformation of load-application structure in real experiment

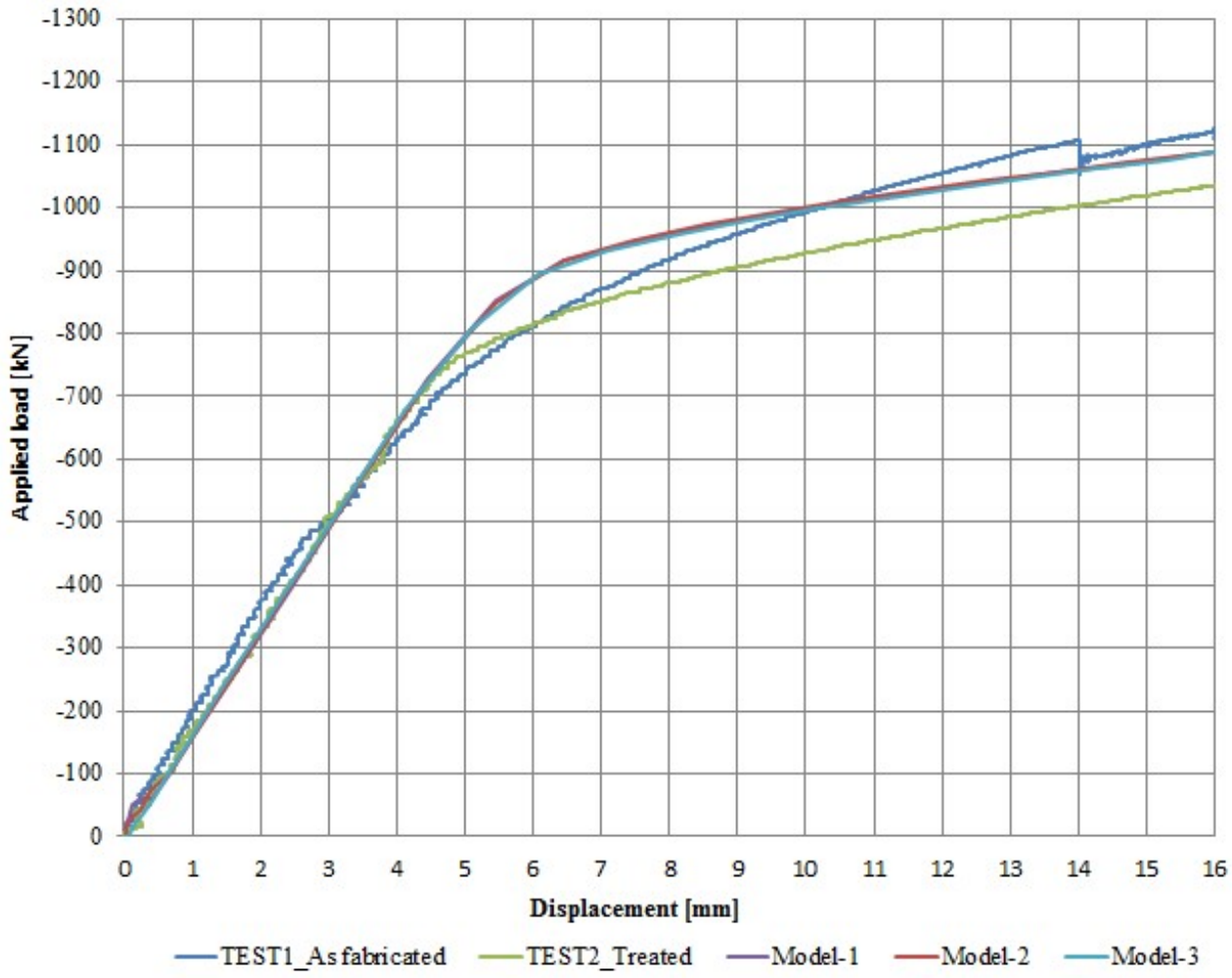

Figure 45. Load-displacement data. Experimental and Numerical modelling data

Analysing the plot, we can see that the linear portion of the curves is pretty consistent, while the actual variations are in the initiation and the trend in the inelastic part. Reason for deviation between experimental results was already discussed in 4.2.4.1.4. It was found that mechanical properties of the material for “as fabricated” and heat-treated rails are different. Ideally, cylinder specimens should be extracted from both rails and tested in order to obtain stress-strain curves. That in turn should be introduced in Abaqus/CAE material plasticity model.

Elastic behaviour of the rail in bending depends mostly on elastic modulus which should not be affected by heat-treatment. Consequently validation of numerical models shall be done for elastic range.

Response of the rail to the same loading level is considered for validation. It is chosen to be 650 kN as it is within elastic range. Corresponding displacement shall be compared and deviation shall be found. Stress levels at the top and bottom of the rail are compared only for

the RO-1 without residual stresses. For RW-1 and RW-2 stresses at the moment of application of load are not equal to 0 as they are for experimental data, so appropriate comparison cannot be made.

Table 11. Validation of RW-1

Experimental	Numerical	Deviation
Displ. [mm]	Displ. [mm]	
4,22	4,05	4%

Table 12. Validation of RW-2

Experimental	Numerical	Deviation
Displ. [mm]	Displ. [mm]	
4,22	4,04	4%

Table 13. Validation of RO-1

	Experimental	Numerical	Deviation
	Stress [MPa]	Stress [MPa]	
Top	-414,54	-449	8%
Foot	436,59	399,45	9%
	Displ. [mm]	Displ. [mm]	Deviation
	4	3,95	1%

Numerical data has a good agreement with experimental data for elastic range.

Validation of the rail behaviour in a plastic range cannot be done in terms of comparison of the displacement or stress values because of uncertain material model. However it is possible to evaluate how correctly the model reproduces real behaviour of the rail in plastic bending. For this purpose Load vs. True strain (Logarifmic strain) plots were constructed. Logarifmic strain is the only possible strain output for Non-linear analysis in Abaqus. Engineering strain (ENG) given as experimental data can be easily converted to logarifmic strain (LE) with following equation:

$$LE = \ln(1 - ENG)$$

Residual stresses in the rail head are tensile while bending stresses there are compressive, so they are subtracted from bending stresses. Consequently, loading that causes yielding of the top fibres is expected to be higher for the specimen with existing residual stresses. We can observe that trend for both numerical and experimental curves presented on Figure 46.

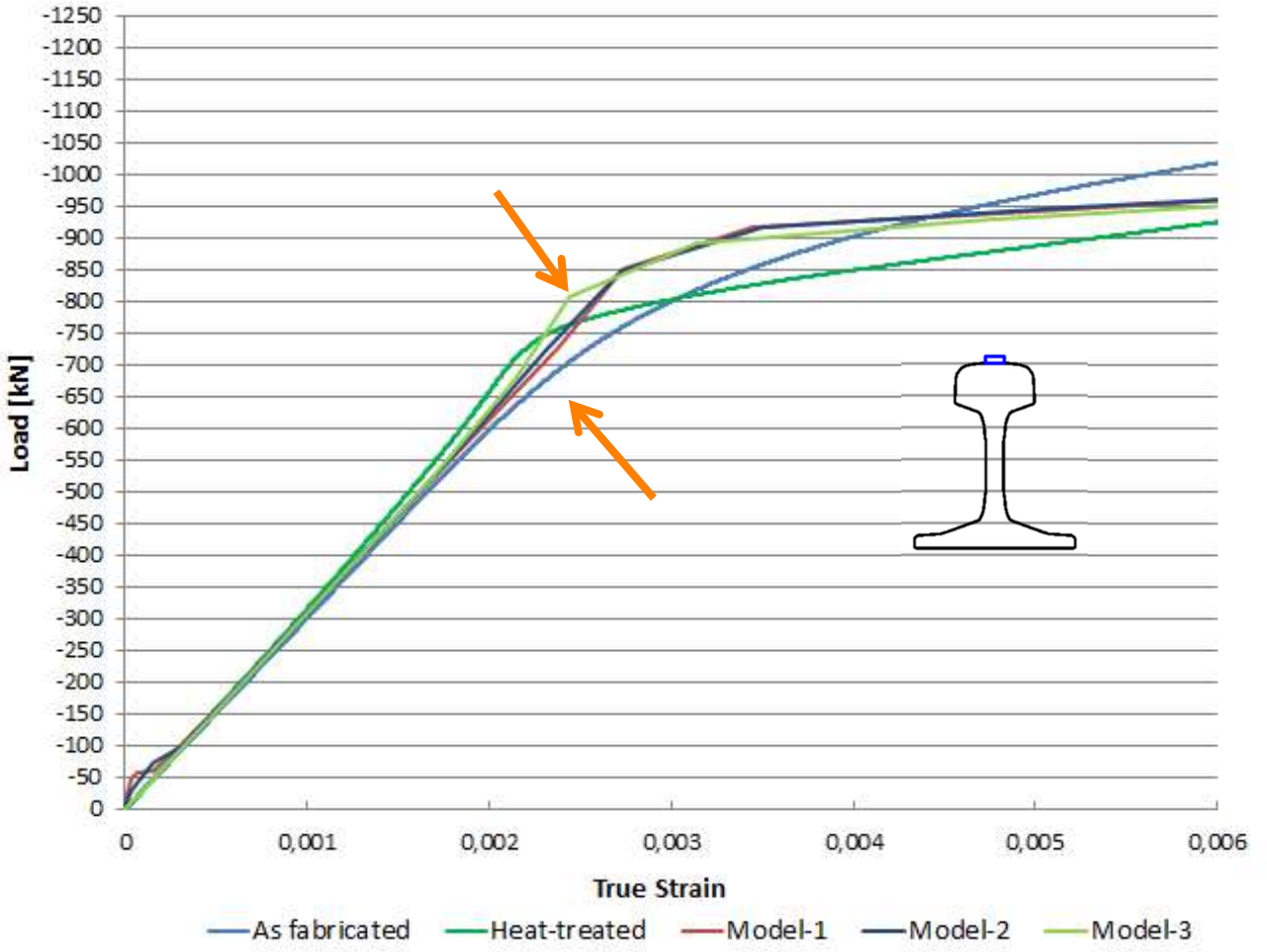

Figure 46. Load vs. Strain plot. Top fibres. RW-1, RW-2, RO-1, experimental data

Contrary to top fibres, bottom fibres experience residual and bending stresses of the same sign. Thus smaller load is needed to cause yielding of the bottom fibres for the specimen with residual stresses. That trend is clear for numerical curves shown on Figure 47. Experimental load-strain curve for “as fabricated” rail is very smooth without well-distinguished yielding point as it is for all steels with high hardness. However similar behaviour to the simulated one can be traced.

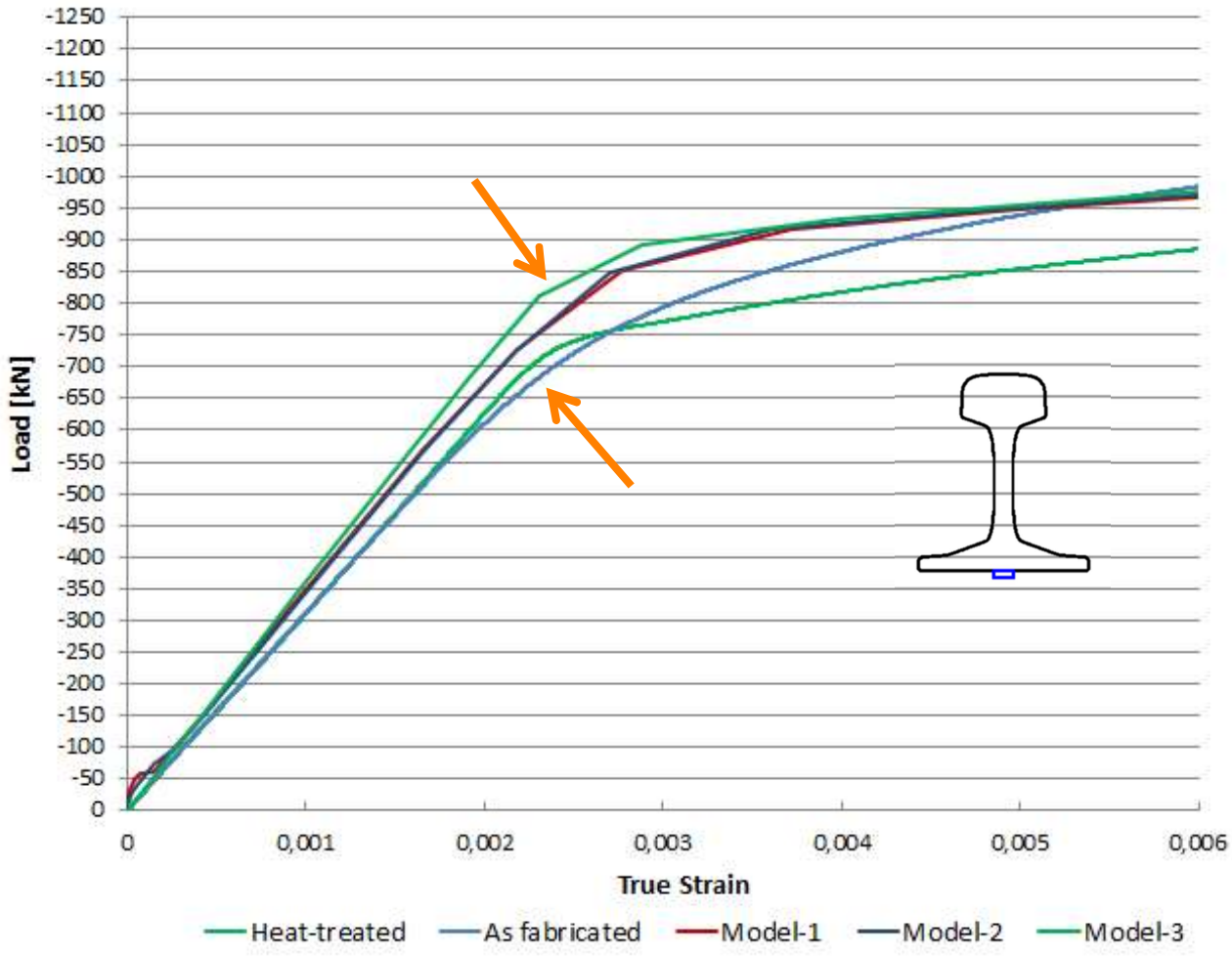

Figure 47. Load vs. Strain plot. Bottom fibres. RW-1, RW-2, RO-1, experimental data

7 FINDINGS

7.1 Influence of residual stresses on static (flexural) behaviour of the rail

Bending analysis was performed for the rail with and without residual stresses ("as fabricated" and heat-treated rails correspondingly). It can be seen from the test results that bending capacity of heat-treated rail specimen is lower than bending capacity of "as fabricated" rail (Figure 48). However it was associated with heat-treatment process where change of material properties took place (4.2.4.1.4 Reason behind deviation). For numerical models material model remains the same, so only residual stresses could cause deviation in results of simulation (Figure 49).

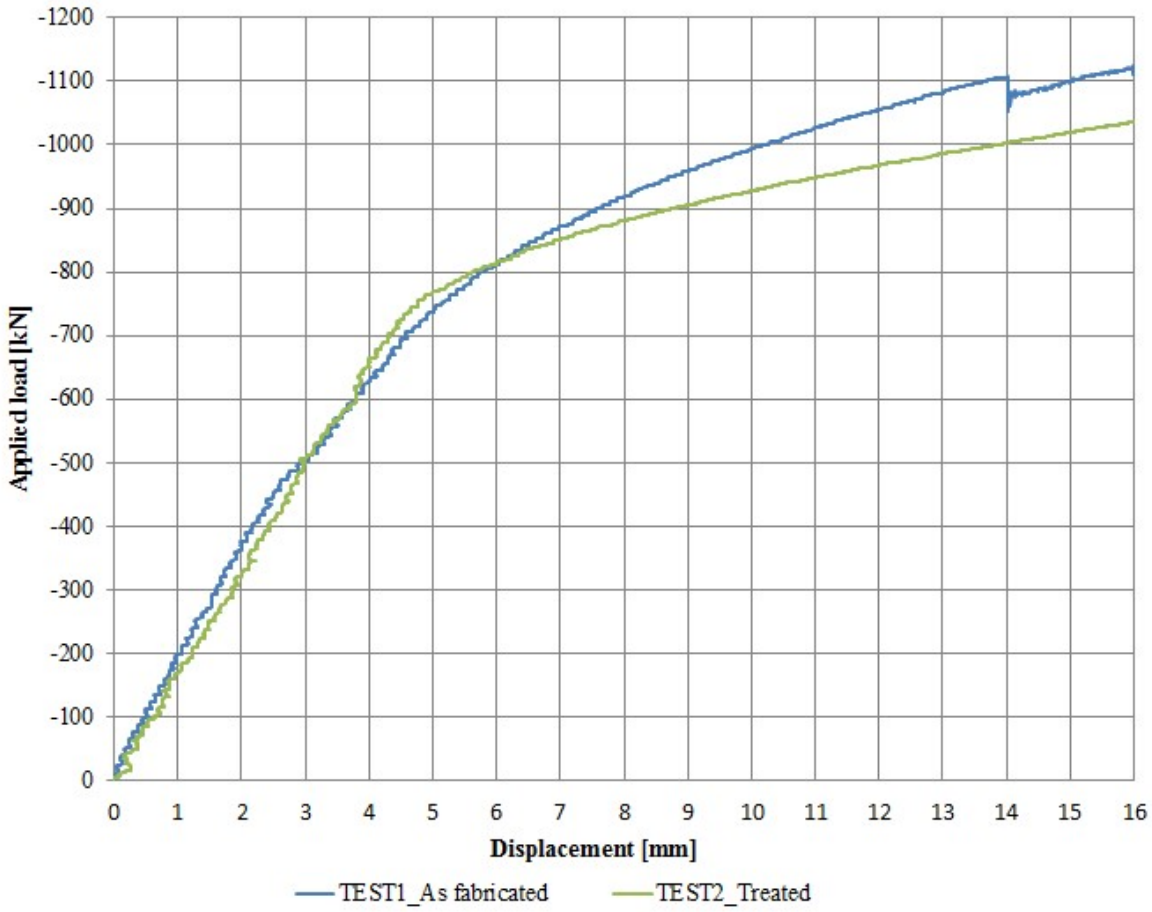

Figure 48. Applied load vs. Displacement of Middle point. Experiment

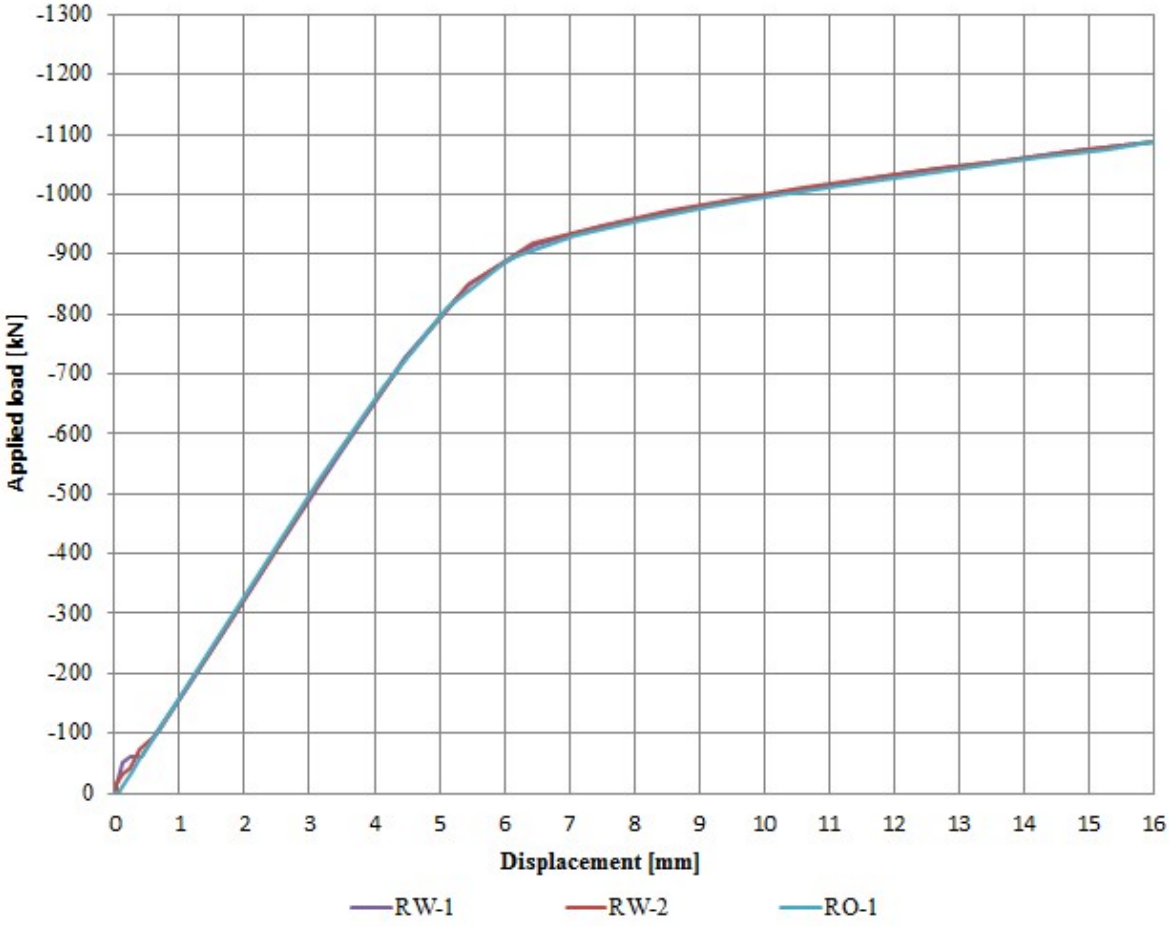

Figure 49. Load vs. Displacement of Middle point. Numerical modelling

All three models exhibit similar flexural behaviour for both elastic and plastic bending. No significant deviation can be observed. Apparently, the reduction in bending load due to tensile residual stresses at the bottom is compensated by the increase in bending load due to tensile stress at the top of the rail. Thus we get approximately same bending load for the cases with and without residual stresses.

Load-unloading cycle was also simulated in order to compare permanent plastic deformation of the bottom fibres in tension for the models with and without residual stresses. Displacement was set to be 10 mm, 3 loading – unloading cycles were applied.

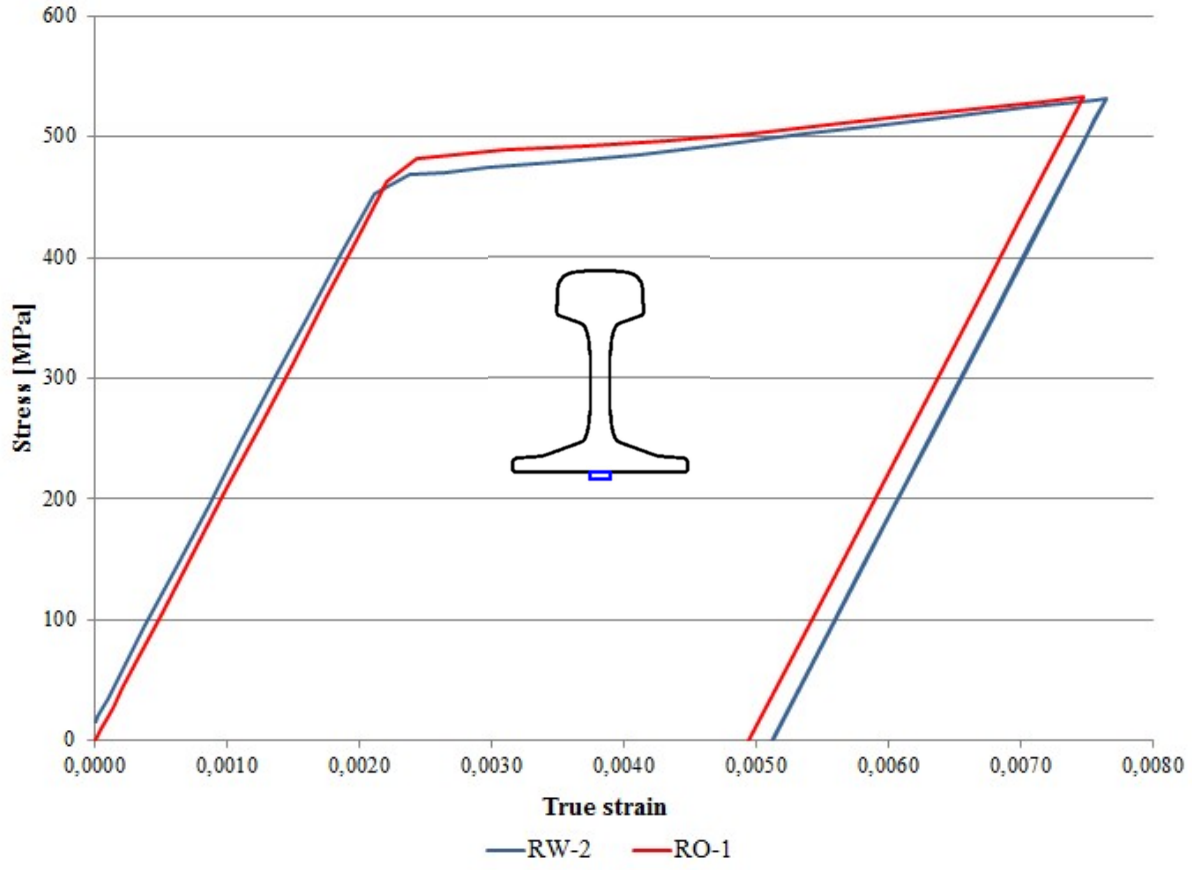

Figure 50. Loading-unloading cycles for displacement 10mm

Permanent deformation for the RW-2 (with residual stresses) is equal to 0.00494, for the RO-1 it is 0.00504. So the difference is 2%.

Consequently, influence of existing residual stresses in rail for performed simulation can be considered neglectable.

7.2 Importance of accurate residual stress pattern

EN 13674-1 controls the maximum tensile stresses in the rail foot below the limit of 250MPa. As it was proved in previous paragraph 7.1, flexural behaviour of the rail is not affected significantly by the residual stresses in it. However surface and near-the-surface residual stresses might have an influence on load that corresponding to yielding of the top and bottom fibres. Foot outer-fibres are in the most unfavourable position because both bending and residual stresses have the same sign.

Three numerical models that were developed in the current work have different residual stress distribution near the surface:

1) RW-1: 130 MPa for the top, 140 MPa for the bottom. Residual stress pattern was taken from the simulation of production process (2.2.3);
2) RW-2: 15 MPa for both top and bottom. Residual stress pattern was based on results of contour method research(2.2.2.3) and IC-DHD technique (2.2.2.4);
3) RO-1: residual stresses were not introduced in that model.

Theoretical assumptions concerning superposition of residual stresses and bending stresses are visualized in stress-strain diagrams presented below.

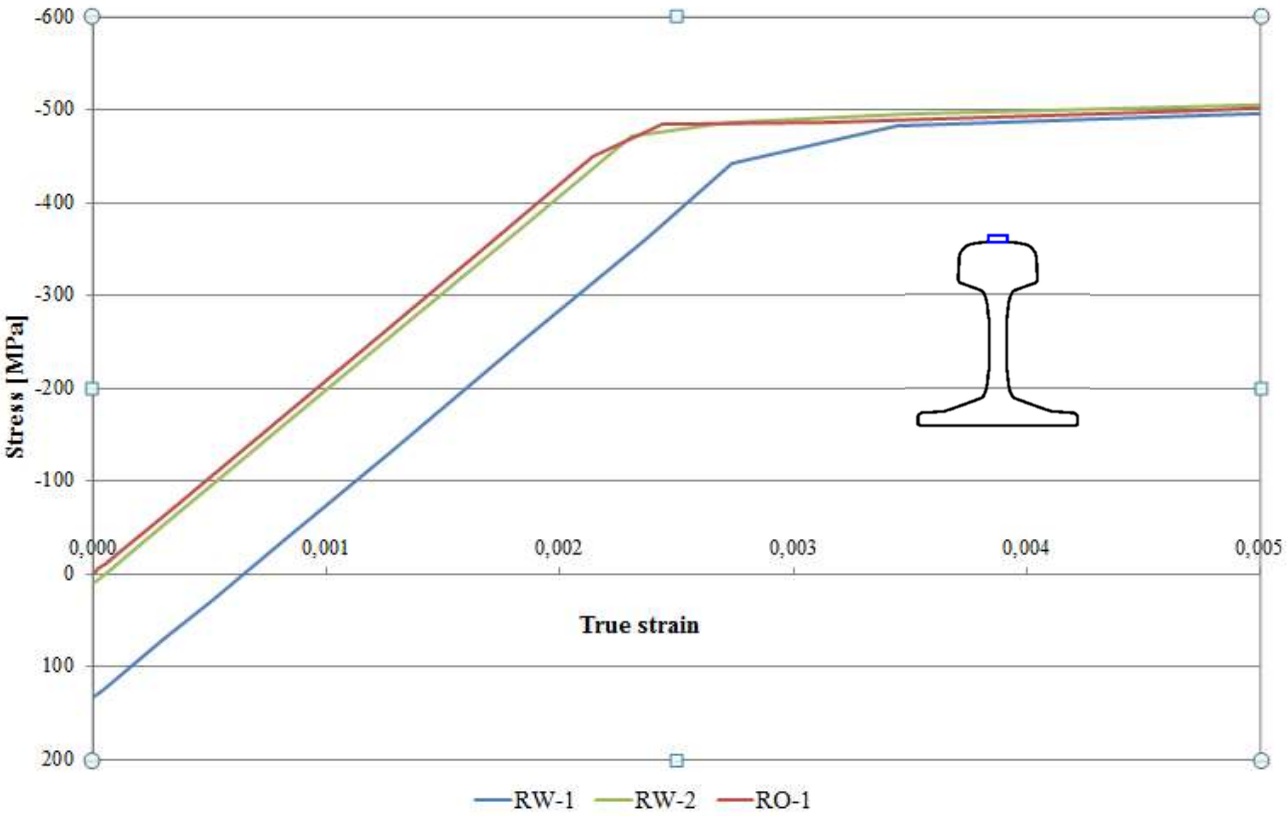

Figure 51. Stress-strain diagram for top fibres. Numerical models

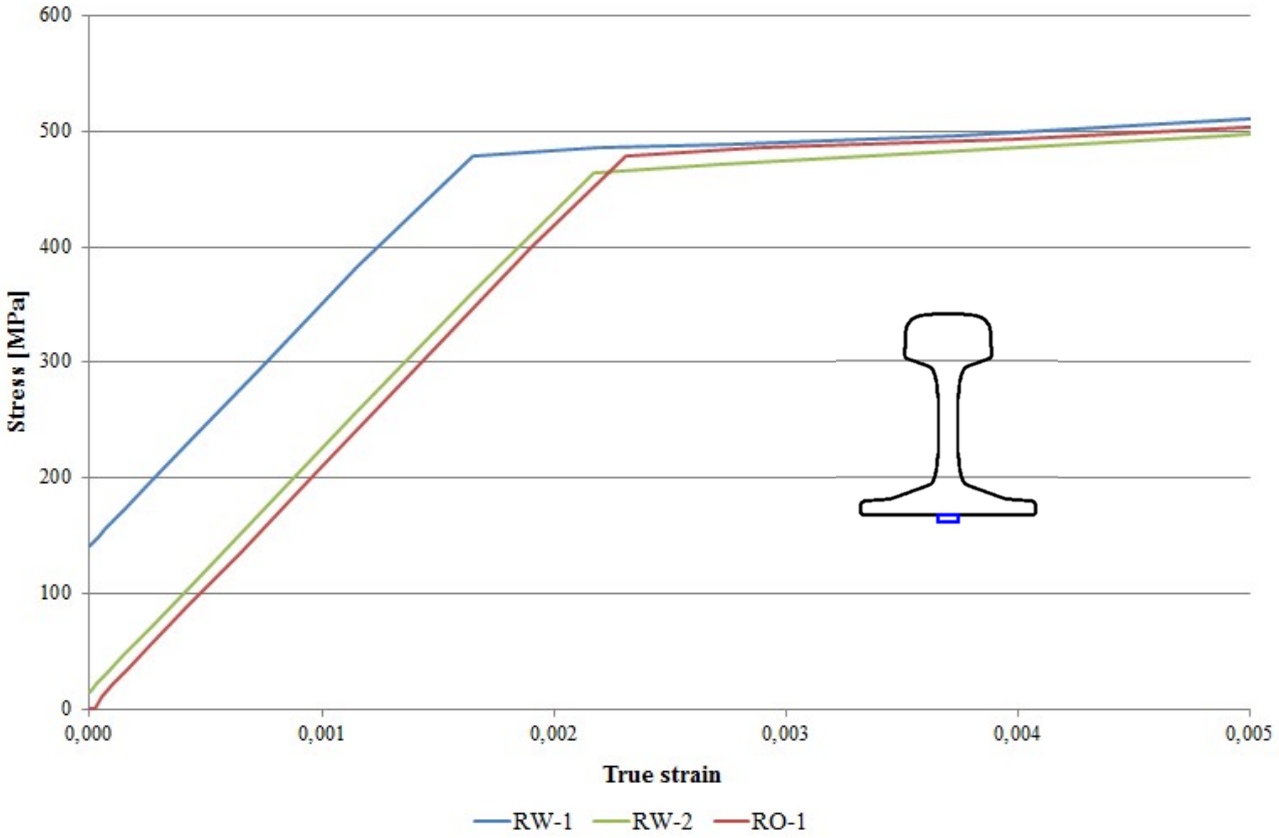

Figure 52. Stress-strain diagram for bottom fibres. Numerical models

Due to existing tensile residual stresses in the top of the rail, higher stress need to be applied to cause yielding of the compressed fibres. Contrary, lower stress is needed to cause yielding of the bottom fibres in tension. Difference between these stresses can be considerable and depends on residual stress pattern used (Figure 51 and Figure 52).

In cases where developing of the plastic strain is under consideration (for instance fatigue resistance), residual stress pattern with refined stress field near the surface should be considered. CHD technique (part of IC-DHD technique 2.2.2.4) can be used in order to add desired accuracy.

FEM simulation of production process gives us global understanding about distribution of residual stresses and their general pattern. Due to some simplifications, especially in defining contact problems, deviations with a real distribution are possible. As an advantage, it provides smooth pattern of residual stresses that can be easily introduced in numerical models for further researches where global behaviour of the rail is under consideration.

Incremental Central and Deep Hole Drilling technique (IC-DHD technique 2.2.2.4) is applied to measure residual stresses locally and can be used for studying critical places of the rail in terms of fracture.

8 FUTURE STUDY

Behaviour of the rail due to vertical central loading was studied. It was concluded that influence of the residual stresses on flexural behaviour of the rail is neglectable.

Moreover because of its shape, the rail is not susceptible to buckling due to bending. Although it may fail due to global or local instability due to longitudinal forces acting on it:

1) Braking/accelerating force from rail transport
2) Temperature load due to temperature variations in the rail

Therefore influence of residual stresses on stability of the track should be further studied. Geometrical imperfections of the rail shall be introduced as well.

9 CONCLUSION

Some rail producers enter the market with heat treated rails aiming reduction of residual stresses in them. Relevance of this is questionable. According to performed study there is no significant benefit of the usage of rails with reduced initial stresses. Both specimens ("as fabricated" and heat-treated) exhibit similar behaviour in elastic range which is a working range for the rails. However we cannot eliminate influence of residual stresses completely. They still play major role in fatigue failure of the rail. What concerns longitudinal resistance of the rail due to track-bridge interaction, existing value accounting residual stresses in rail is set as 100 MPa in MVL-150 [3]. One the one hand, it cannot be reduced until research for the stability of the track is done. One the other hand, presented work doesn't provide reasons for increasing considered value of residual stresses in railway rail UIC60.

10 REFERENCES

[1]. Timoshenko, S. and B.F. Langer, Streees in railroad track. ASME, 1931

[2]. Union Internationale des Chemins de fer (UIC), 774-3R. Track/bridge interaction, Recommendations for calculations, Paris, 2001.

[3]. MVL 150, KOMBINOVANÁ ODEZVA MOSTU A KOLEJE, Správa železniční dopravní cesty

[4]. Handbook of Residual Stress and Deformation of Steel. Materials Park, US: ASM International, 2002. p.424-436 Residual stress formation and distortion of Rail steel. F.D. Fischer and G. Schleinzer, Insitut fur Mechanik, Institute of Mining and Metallurgy, Montanuniversit at Leoben, Franz-Josef-Strasse 18A-8700 Leoben, Austria

[5]. Residual stress formation during the roller straightening of railway rails. G. Schleinzer, F.D. Fischer, Insitut fur Mechanik, Institute of Mining and Metallurgy, Montanuniversit at Leoben, Franz-Josef-Strasse 18A-8700 Leoben, Austria. Received 31 March 2000; received in revised form 12 January 2001

[6]. Residual Stress Measurement within an European UIC60 Rail Using Integrated Drilling Techniques, D. Stefanescu, P. Browne, C. E. Truman and D. J. Smith. University of Bristol, Department of Mechanical Engineering, Queen's Building, University Walk,Bristol, BS8 1TR, United Kingdom,Balfour Beatty Rail, Midland House, Derby, DE1 2SA, United Kingdom

[7]. P.J. Webster, X. Wang, G. Mills and G.A. Webster: Physica B, Vols. 180-181 (1992), p. 1029 “Residual stress changes in railway rails”

[8]. The measurement of residual stress in railway rails by diffraction and other methods. J Kelleher (Manchester Materials Science Centre), Michael B. Prime (ESA-WR),D Buttle (AEA Technology plc), P M Mummery (Manchester Materials Science Centre), P J Webster (FaME38 at ILL-ESRF), J Shackleton (Manchester Materials Science Centre), P J Withers (Manchester Materials Science Centre). Journal of Neutron Research, 11(4), 187-193, 2003.

[9]. C. O. Ruud. A review of selected non-destructive methods for residual stress measurement. NDT International 1982; 15(1): 15-23

[10]. Studies Concerning the Measurement and Improvement of the Level of Residual Stresses, ORE D 156/Report 4, Utrecht, the Netetherlands, 1987

[11]. W.H. Hodgson, Residual Stresses in Rail. Rail Quality and Maintenance for Modern Railway Operation, pp 61-73, Kluwer Academic Publishers, the Netherlands, 1993

[12]. J.L. Chaboche, Constitutive Equations for Cyclic Plasticity and Cyclic Viscoplasticity, Int. J. Plast, Vol. 5, 1989

[13]. Correlation of Yield Strength and Tensile Strength with Hardness for Steels. Pavlina, E. & Van Tyne, C. J. of Material Eng. and Perform (2008) 17: 888.

[14]. Investigation of the stresses in rails: Secondary effects associated with the bending of a centrically loaded rail, AJ Kolvoort, T Woestenburg - HERON, 27 (2), 1982

[15]. J. Eisenmann, Theoretical considerations on the stress conditions in the rail head at the point of load application, Technological University of Munich, 1965

11 ANNEXES

ANNEX 1 RAIL PROFILE 60E1 – DIMENSIONS (EN 13674-1:2011)

Dimensions in millimetres

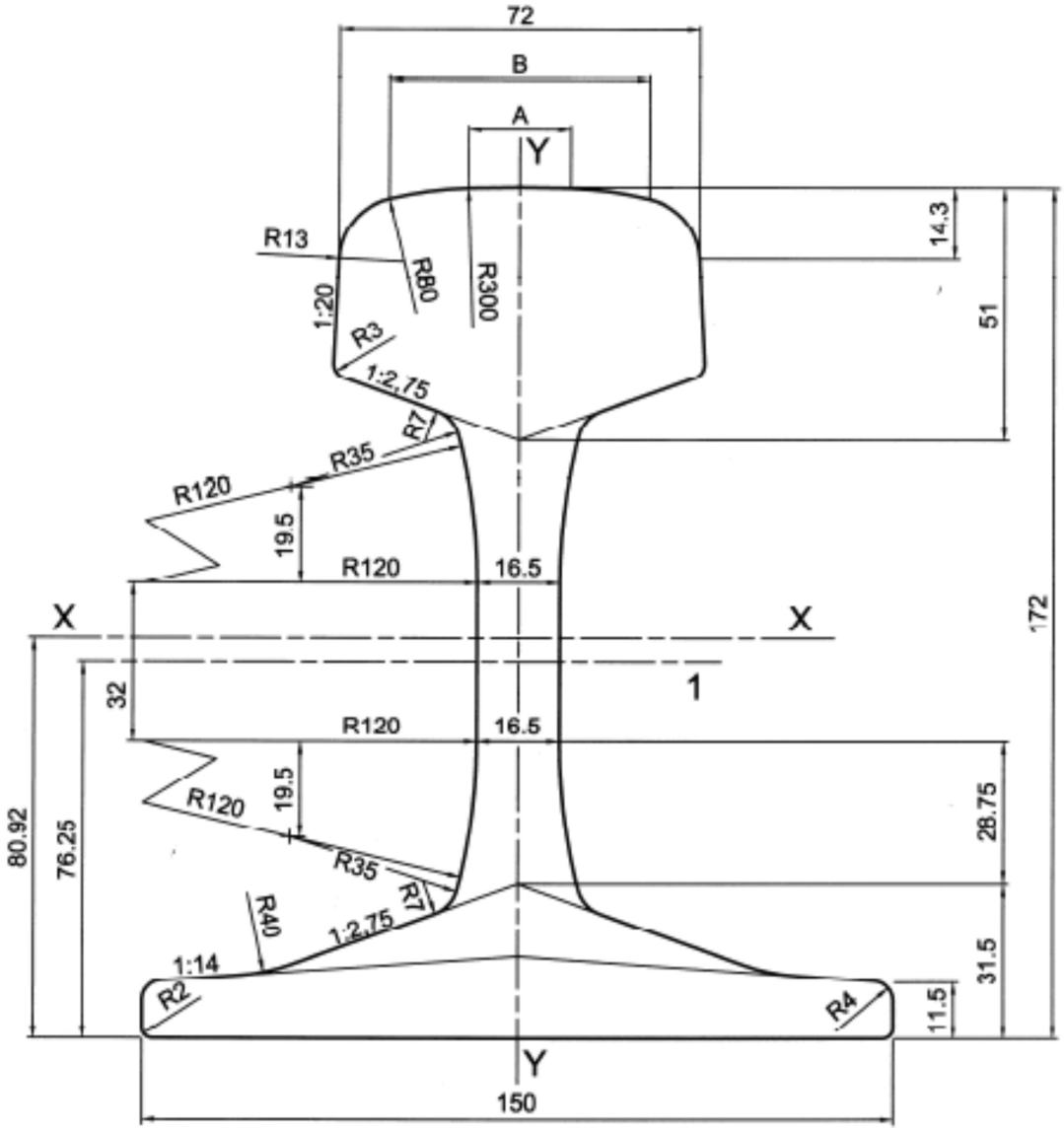

Key

1 centre line of branding

cross-sectional area	:	76,70	cm^2
mass per metre	:	60,21	kg/m
moment of inertia x-x axis	:	3 038,3	cm^4
section modulus - Head	:	333,6	cm^3
section modulus - Base	:	375,5	cm^3
moment of inertia y-y axis	:	512,3	cm^4
section modulus y-y axis	:	68,3	cm^3

indicative dimensions: A = 20,456 mm
B = 52,053 mm

Annex 2 Quality certification protocol for purchased rail pieces

Správa železniční dopravní cesty

Správa železniční dopravní cesty, státní organizace
TECHNICKÁ ÚSTŘEDNA DOPRAVNÍ CESTY
Kvalita a použitelnost materiálu
Riegrovo náměstí 814
500 02 Hradec Králové

Protokol o ověření kvality

číslo: 1-Amko/2015

Výrobce-prodávající:
ARCELOR MITTAL, Arcelor Mittal Poland S.A,
Al. J. Piłsudskiego 92,
41- 308 Dabrowa Gornicza

Kupující: (obchodní jméno, adresa)
STRABAG Rail a.s.
Železničářská 1385/29
400 03 Ústí nad Labem-Střekov

Číslo kupní smlouvy/číslo zakázky:
10548665/1

Místo určení dodávky:
Chabařovice

Číslo smlouvy o kontrolní činnosti:
E791-S-1066/2014

Místo provedení ověření kvality:
Arcelor Mittal Poland Dabrowa Gornicza

Ověřovaný materiál (výrobek)

Název-popis materiálu (výrobku)
Kolejnice tv. 60E2 R260
120 m - 108 ks

Množství:
777 988

Měrná jednotka:
kg

Výrobní číslo:

Ověření kvality provedeno podle:
EN 13674-1:2011
TPD 1/2012 + Dodatek č.1

Předložené doklady o zkouškách a atesty materiálu:
Inspekční certifikát 3.1 č. 1/2015

Výsledek ověření kvality:
vyhovuje

Ověřené výrobky jsou ~~nejsou~~ označeny značkou kontrolora sždc-4

Přílohy tohoto protokolu:
Inspekční certifikát dle EN 10204 -3.1

Jméno kontrolora:
Roman Rožycki

Datum:
15.1.2015

Razítko a podpis výrobce-prodávajícího:

Razítko a podpis kontrolora kvality SŽDC:

Tento evidenční výtisk slouží pouze pro potřeby archivace a nikoli jako doklad o ověření kvality uživatelem pověřeným orgánem.

SŽDC KPM 2/11

A01-Zakład wytwórczy/Manufacturer's works	A02-Rodzaj dokumentu kontroli/ Type of inspection document	A03-Numer dokumentu/ Document number	A05.1-Wystawiający dokument/Originator of the document
ArcelorMittal **ArcelorMittal Poland S.A.** Oddział w Dąbrowie Górniczej Al. J. Piłsudskiego 92 41-308 DĄBROWA GÓRNICZA POLAND	**ŚWIADECTWO ODBIORU 3.1** **INSPECTION CERTIFICATE 3.1** **EN 10204:3.1**	**No 1/2015**	**GJ-3** **Kontrola Jakości - wyroby długie** GJ-36 Certyfikacja Wyrobów i Dokumentacji Kontrolnej A02.1-Data/Date 09.01.2015

FIRMA POSIADA CERTYFIKAT WYDANY PRZEZ TÜV CERT NA SYSTEM JAKOŚCI ZGODNY Z NORMĄ EN ISO 9001
QUALITY SYSTEM OF OUR COMPANY HAS BEEN CERTIFIED BY THE TÜV CERT ACC. EN ISO 9001

A06-Zamawiający / Customer	**Strabag Rail a.s. Zeleznicarska 1385 29 400 03 Usti nad Labem-Strekov, CZ**
A06- Odbiorca / Consignee	**Strabag Rail a.s. Zeleznicarska 1385 29 400 03 Usti nad Labem-Strekov, CZ**

A07-Numer zamówienia klienta/ Purchaser's order number	A08-Nr zamówienia zakładu wytwórcy/Manufacturer's works order number	A10-Nr dowodu dostawy/ Advice No	A11-Nr wagonu/Wagon No	A12-Kod PKWiU/ CTWH Code PKWiU/ CTWH
	10548665/1			

Wyszczególnienie zamówienia - Order Specification

B01-Wyrób/ Product B04-Stan dostawy wyrobu/Product delivery condition	B06-B11-Wymiary wyrobu/ Product dimensions [mm]	B02-Gatunek stali/Steel designation	B07-Identyfikacja wyrobu/identification of the product Nr wytopu / Heat No	B08-Liczba sztuk/ Number of pieces	B12-Masa teoretyczna/Theoretical mass kg	B13-Masa rzeczywista /Actual mass kg
RAILS 60E2 AX EN 13674-1:2011 TPD 1/2012+Dodatek 1	**60E2 x 120000**	**R260**	**510045(T379); 510026(T380); 520050(T381); 510030(T382); 520022(T383); 510056(T384).**	**108**	**777.988,800**	-

C71 - SKŁAD CHEMICZNY - CHEMICAL COMPOSITION

B03-Nr wytopu / Heat No	C	Mn	Si	P	S	H_2	O_2
	x0,01 [%]			x0,001 [%]		ppm	ppm
Specification of rails Reserch results No 1/2015							

C12 - C16 - BADANIA MECHANICZNE - MECHANICAL TESTS

C12/C13/C14-Próba rozciągania/ Tensile test				C15-Twardość Brinella/ Brinell Hardness		C16-Próba Kafarowa/ Falling weight test
Nr czyny / Reel No	Rm MPa	A %	Z %	Nr czyny / Reel No	HB	Nr czyny Strzałka ugięcia / Reel No Deflection mm
Specification of rails Reserch results No 1/2015						

C17-C20 - BADANIA METALOGRAFICZNE - METALLOGRAPHIC TESTS

B07-Nr wytopu / Heat No	C17-Próba Baumana/ Baumann test		C18-Mikrostruktura/ Microstructure		C19-Odwęglenie/ Decarburization		C20-Wtrącenia tlenkowe/ Oxide inclusions	
	Nr czyny / Reel No	Nr wzorca / Standard No	Nr czyny / Reel No	Ocena / Mark	Nr czyny / Reel No	Głębokość / Depth [mm]	Nr czyny / Reel No	KJ DW 35602
Specification of rails Reserch results No 1/2015								

D81 - INNE BADANIA - OTHER TESTS

UT - TESTING IN 100%
WADY MIKROSKOPOWE ZBADANO W 100%

Powierzchnię i wymiary zbadano / Surface and dimension tested: w 100% / in 100%

B06-Oznakowanie wyrobu/Marking of the product

Z01-Stwierdzenie o zgodności: Producent deklaruje, że dostarczone wyroby są zgodne z warunkami zamówienia / Statement of compliance: The producer guarantees that the delivered goods are in accordance with the conditions of the order

A05.2-Certyfikacja Wyrobów i Dokumentacji Kontrolnej/ Certificate Section	Z02.2- Główny Specjalista Certyfikacji Wyrobów i Dokumentacji Kontrolnej/ Chief Specialist Certificate Section
Sporządził/ Prepared by: (-) Sprawdził/ Checked by: (-) Antoni Czechowski I Specjalista Kontrola Jakości wyroby długie Certyfikacja Wyrobów i Dokumentacji Kontrolnej	Główny Specjalista ds. Certyfikacji Wyrobów i Dokumentacji Kontrola wyroby długie Zdzisław Kapinski

EN 10168:2004

Zestawienie wyników badań szyn / SPECIFICATION OF RAILS' RESERCH RESULTS / ÜBERSICHT DER SCHIENENPRÜFERGEBNISSE Nr / No / NR: 1/2015
Oznaczenie stali / STEEL DESIGNATION / STAHLSORTEKENNZEICHNUNG : R260
Identyfikacja wyrobu / IDENTYFICATION OF THE PRODUCT / PRODUKTIDENTIFIZIERUNG: 60E2

Lp. No.	Nr wytopu Heat No Abstich	Nr kodu wyrobu Code of Iron Abstich	Nr wzoru Rail No. scheme Nr	Analiza chemiczna wytopu Chemical Analysis of heat Chemische Zusammensetzung																						
				C %	Mn %	Si %	P %	S %	Cr %	Ni %	Cu %	Al %	N2 %	Mo %	As %	Ti %	Ca %	Pb %	Sn %	Sb %	O2 %	H2 %	Zn %	W %	Nb %	V %
1	2	3	4	5	6	7	8	9	10	11	12	13	14	15	16	17	18	19	20	21	22	23	24	25	26	27
1	510045	T378		0,70	1,08	0,33	0,012	0,018	0,04	0,01	0,03	0,001	0,0006	0,005	0,002	0,0010		0,0010	0,0020	0,0010	0,0018	0,00011	0,0001	0,0010	0,0018	0,0038
2	510038	T380		0,74	1,09	0,34	0,011	0,014	0,04	0,02	0,03	0,001	0,0057	0,002	0,002	0,0010		0,0010	0,0030	0,0010	0,0018	0,00011	0,0001	0,0010	0,0006	0,0040
3	520095	T381		0,73	1,08	0,32	0,011	0,013	0,03	0,01	0,02	0,002	0,0054	0,001	0,001	0,0010	0,0001	0,0010	0,0040	0,0010	0,0018	0,00013	0,0001	0,0010	0,0001	0,0049
4	510030	T382		0,74	1,08	0,32	0,013	0,017	0,04	0,03	0,03	0,001	0,0046	0,005	0,002	0,0010		0,0010	0,0030	0,0010	0,0014	0,00013	0,0001	0,0010	0,0006	0,0034
5	520072	T382		0,74	1,08	0,33	0,012	0,014	0,05	0,01	0,03	0,003	0,0087	0,004	0,002	0,0010		0,0010	0,0030	0,0010	0,0018	0,00011	0,0004	0,0010	0,0006	0,0038
6	510016	T384		0,74	1,09	0,33	0,010	0,014	0,04	0,01	0,02	0,003	0,0059	0,002	0,001	0,0010	0,0001	0,0010	0,0030	0,0010	0,0012	0,00011	0,0001	0,0010	0,0002	0,0043

Główny Specjalista
ds. Certyfikacji Wyrobów i Dokumentacji
Kontrolnej [illegible]
Zdzisław Kopański

Strona 1/2

ANNEX 3 ACCOUNTING ON ADDITIONAL VERTICAL DISPLACEMENT

Displacement sensors U1, U2 and U3 capture total displacement. Due to the applied load, local crashing of steel on the surface of the supports occurs which should be excluded from the total displacement. This crashing is considered to progress during experiment until certain limit of 1.6 mm. Maximum crashing was instrumentally measured after reassembling setup of the test after it was finished.

Since main behaviour of the rail can be described according to the beam theory [14], displacement due to rotations of the beam ends (Ur) can be calculated and displacement due to crashing (Uc) shall be separated from the displacements U2 and U3.

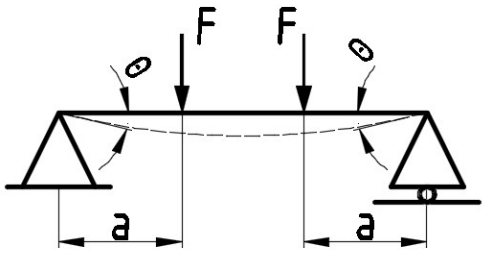

For four-point bending angle of rotation is calculated according to following equation:

$$\theta := \frac{F \cdot a \cdot (L - a)}{2E \cdot I}$$

Displacement is therefore:

$$u_r := \theta \cdot 70mm$$

where 70 mm is a distance from the support to the displacement sensors U2 (U3).

As there is some deviation between U2 and U3 measurements, average value of Uc was calculated:

$$u_c = \frac{(u_2 + u_3)}{2} - u_r$$

$$u_c \leq 1.6mm$$

Absolute displacement of the middle point of the rail Um can be finally found:

$$u_m = u_1 - u_c$$